

# From Large to Super-Tiny: End-to-End Optimization for Cost-Efficient LLMs

Jiliang Ni\* Jiachen Pu\* Zhongyi Yang\* Kun Zhou Hui Wang  
 Xiaoliang Xiao Dakui Wang Xin Li Jingfeng Luo Conggang Hu†  
 Intelligent Connectivity  
 Alibaba Group  
 conggang.hcg@alibaba-inc.com

## Abstract

In recent years, Large Language Models (LLMs) have significantly advanced artificial intelligence by optimizing traditional Natural Language Processing (NLP) pipelines, improving performance and generalization. This has spurred their integration into various systems. Many NLP systems, including ours, employ a "one-stage" pipeline directly incorporating LLMs. While effective, this approach incurs substantial costs and latency due to the need for large model parameters to achieve satisfactory outcomes. This paper introduces a three-stage cost-efficient end-to-end LLM deployment pipeline—including prototyping, knowledge transfer, and model compression—to tackle the cost-performance dilemma in LLM-based frameworks. Our approach yields a super tiny model optimized for cost and performance in online systems, simplifying the system architecture. Initially, by transforming complex tasks into a function call-based LLM-driven pipeline, an optimal performance prototype system is constructed to produce high-quality data as a teacher model. The second stage combines techniques like rejection fine-tuning, reinforcement learning, and knowledge distillation to transfer knowledge to a smaller 0.5B student model, delivering effective performance at minimal cost. The final stage applies quantization and pruning to extremely compress models to 0.4B, achieving ultra-low latency and cost. The framework's modular design and cross-domain capabilities suggest potential applicability in other NLP areas.

## 1 Introduction

In recent years, Large Language Models (LLMs) have made significant strides [1; 2; 3] in enhancing artificial intelligence by addressing shortcomings of traditional pipelines — including manual annotation, suboptimal performance, and limited generalization and adaptability. Consequently, LLM-based pipelines have stimulated substantial demand for integration into various Natural Language Processing (NLP) systems. We find that numerous NLP systems, including our own, have directly adopted LLM into the pipeline, often referred to as the "one stage"

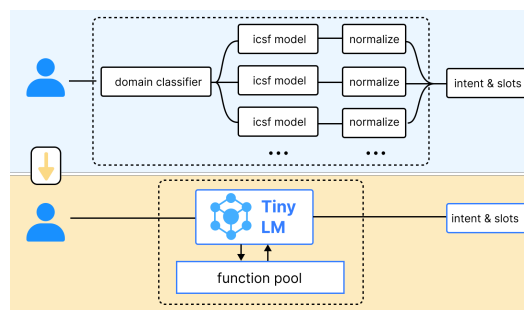


Figure 1: From the traditional BERT-based system to the LLM-based system.

\* Equal Contribution

† Corresponding Author

pipeline. Despite the breakthroughs facilitated by this pipeline, it also incurs substantial cost increases [4] and high inference latency [5]. Within our NLP system, cost-performance is an especially critical metric, a sentiment likely shared by others in the field [6]. These significant costs limit the broader applicability of LLMs and impact their commercial viability. Our analysis points out that it is precisely the simplistic training method of the one-stage pipeline, which necessitates larger model parameters to achieve satisfactory results, that leads to significant costs.

In this paper, we introduce a three-stage performant and cost-efficient end-to-end LLM deployment pipeline, consisting of prototyping, knowledge transfer, and model compression, to address the pervasive "cost-performance" dilemma in the practical deployment of LLM-based frameworks. This approach ultimately yields a super tiny model, which is deployed in our online system, achieving optimal cost-performance metrics while substantially simplifying system architecture. The first stage involves constructing the prototype system, where traditional complex tasks are converted into function call-based LLM-driven workflows [7] through prompt engineering, resulting in an optimal performance prototype compared to traditional pipeline. This prototype serves as a teacher model in the second stage, efficiently generating vast quantities of high-quality data. During the knowledge transfer phase, leveraging the optimal prototype from the first stage, we employ techniques including rejection fine-tuning (RFT), reinforcement learning (RL) [8; 9; 10], and multi-strategy knowledge distillation (KD) targeting the Qwen 2.5 series model [11], effectively transferring knowledge to a 0.5B student model. The derived student model is considerably smaller than the prototype model while achieving nearly comparable performance at minimal cost. In the third stage, we utilize quantization and pruning techniques to further compress the student model developed in the second phase, resulting in a remarkably compact model of 0.4 billion parameters (as shown in Figure 1). Ultimately, this super tiny model is deployed in our online system. This model achieves hundreds-fold compression and extremely low latency and cost in exchange for a trivial and acceptable loss in performance. The modular design and superior cross-domain performance of the framework suggest its potential applicability in other NLP domains. The major contributions of this paper are as follows:

- The first validated three-stage cost-efficient end-to-end LLM pipeline with simplifying original system complexity achieves SOTA results and resolves the "cost-performance" dilemma, realizing a 180-fold compression with nearly consistent AR compared to 72B LLMs and up to an absolute 14% AR increase compared to traditional BERT-based pipelines.
- We propose the first hybrid strategy that significantly enhances the generalization of super tiny models on domain-specific tasks through combining RL and KD. This approach effectively transfers the capabilities of LLMs to smaller models.
- The proposed framework offers advantages such as low training, inference, and deployment costs, minimal project development expenses with fast cycles, and a strong potential for cross-domain transferability. It provides inspiration for developing standardized cross-domain solutions in both academia and industry, facilitating the widespread LLMs adoption.

## 2 Related Works

**LLM for Function Calling & Evaluation** Leveraging in-context learning and reasoning capabilities, LLMs can select functions and parameters from provided lists based on user intent [12]. Fine-tuned 7B models like Gorilla [13] achieve GPT-4-level Function Call accuracy on datasets with thousands of APIs. Building on this, TinyAgent [14] enables function calling capabilities for edge devices with sub-1.1B parameter models. Query-to-API reformulation via rejection sampling can also optimize API retrieval, reducing retrieval latency while improving accuracy [15]. Nowadays, LLMs can be used to evaluate model-generated content [16; 17]. CriticGPT [18] indicates that LLMs can build a cost-effective and high-precision judge, surpassing humans in detecting subtle errors.

**Knowledge Distillation** Knowledge distillation (KD) [19] transfers knowledge from a teacher model to a smaller student model by simulating probability distribution. Common approaches include Logits-based [20; 21], Feature-based [22] and sequence-level (Seq-KD) [23] distillation. Initially, Logits-based KD uses the forward KL divergence (FKL) [24; 25] as the loss function. Some KD methods prefer Reverse KL divergence (RKL) [26; 27; 28; 21]. Recently, Adaptive Kullback-Leiber (AKL) divergence [29] achieves a balance between mimicking distribution and avoiding overfitting.

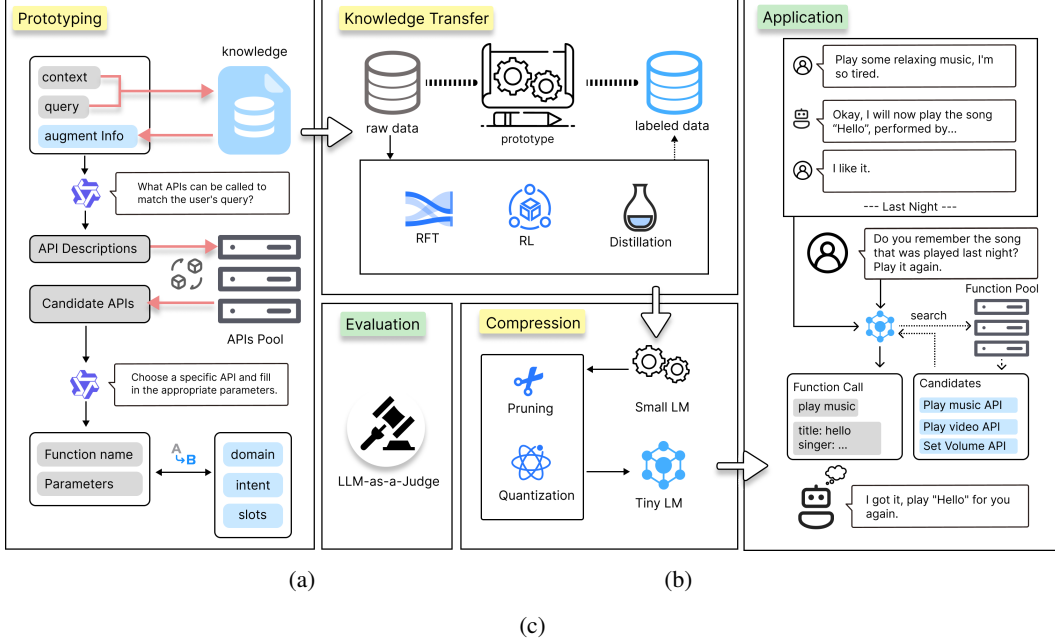


Figure 2: Overview of Prototype, Production and Application.

**LLM Pruning & Quantization** Efficient LLM deployment primarily relies on pruning[30; 31] and quantization[32; 33; 34]. Structured pruning[35] employs layer removal[36; 37] or dimensionality reduction[31; 37; 38] using gradient-based[31; 38] or activation-aware[37] importance criteria, implemented via learnable masks[38; 39] or pruning-retraining pipelines[36; 31; 37]. Weight-only LLM quantization methods[32; 33; 40] improve memory efficiency while joint weight-activation schemes[34; 41] and their combination [42] accelerate computation.

**Reinforcement Learning** Recent works [8; 9; 10] focus on leveraging Reinforcement Learning (RL) to enhance model reasoning capabilities. Notable reasoning models such as DeepSeek-R1 [43], QWQ-32B [44], and OpenAI o1 [45] have emerged, employing RL algorithms like Proximal Policy Optimization (PPO) [46], Group Relative Policy Optimization (GRPO) [47], and others [48; 49; 50]. For general-purpose LLMs, preference optimization algorithms [51; 52; 53; 54] are widely adopted. Additionally, self-improving pipelines [55; 56; 57] have been proposed to iteratively refine model performance. We primarily utilize RL to enhance the model’s generalization. Compared to directly distilling a reasoning model, RL results in shorter and more precise Chains-of-Thought (CoT).

### 3 Methodology

Recent advancements in LLMs have facilitated significant progress in NLP tasks such as classification and summarization. We harness these capabilities to reconstruct the traditional dialogue system through a cost-efficient end-to-end LLM pipeline, which includes prototyping, knowledge transfer, and model compression, as illustrated in Figure 2a and Figure 2b. Initially, we develop the prototype system by leveraging the exceptional performance of contemporary LLMs. Subsequently, we perform knowledge transfer from large models to smaller models. Finally, we achieve additional reduction in model size through further model compression techniques. Ultimately, our objective is to deliver intelligent user experiences at minimal costs, as demonstrated in Figure 2c.

#### 3.1 Prototyping

**LLM Prototype** Traditional dialogue systems usually employ the Intent Classification and Slot Filling (ICSF) framework, often utilizing BERT[60; 61]. However, a single model often struggles to handle complex real-world issues, as shown in the Table 1. Consequently, a Domain Classifier (DC) is frequently used to first categorize queries into domains, enabling domain-specific ICSF

Table 1: Complexity statistics of Our dataset vs Open Source datasets. More details in [Appendix A](#).

Dataset	Test Set Size	Intents	Slots	TTR	Entropy
TinyAgent[14]	1023	17	48	0.0087	7.8220
Snips[58]	893	7	72	0.0207	7.6997
ATIS[59]	700	21	120	0.0111	7.4148
Our dataset	11922	74	225	0.1410	9.4250

parsing. Although the hierarchical DC-ICSF architecture improves accuracy, the system complexity increases with feature updates. This leads to high inter-module coupling, increasing development and maintenance costs. Furthermore, ambiguous domain boundaries turn the DC into a bottleneck for overall end-to-end accuracy, creating a "feature expansion - operational difficulty" feedback loop that hinders dialogue experience optimization.

Modern LLMs exhibit adequate capability to tackle these NLP problems. Particularly in related Tool Use works, LLMs can learn to call functions without additional training by attaching function descriptions in prompts. Essentially, ICSF can be viewed as a function call task, where the model extracts critical information from user queries as function parameters for specific modules to execute. Following this approach, we design a prototype system based on Qwen2.5-72B-Instruct[11]. As illustrated in [Figure 2a](#), the prototype system accepts user queries and contextual information (including chat history and temporal status information) as input, searches relevant APIs from the API pool, then outputs function names and parameters to call. The traditional system comprises one DC module and multiple ICSF models (based on BERT or regular expressions), each requiring separate maintenance and frequent DC updates. In contrast, the LLM-based system, equipped with function call capability, processes all tasks through a unified model, as illustrated in [Figure 1](#), thereby reducing system complexity and enhancing operational efficiency.

To enhance temporal awareness and mitigate hallucinations, we enrich the input with contextual knowledge via RAG [62], retrieving explanations and extensions of entity-related terms from a curated knowledge base. Instead of adding all callable APIs from the API pool into the LLM prompt, we implement an API retrieval module inspired by [15]. The LLM first generates potential API descriptions, then retrieves top-K APIs via vector similarity (using GTE-Qwen2-1.5B [63] as the embedding model and FAISS [64] for indexing). Then, the LLM selects optimal functions/parameters from candidate APIs. If no suitable function exists, the system returns "No appropriate function"; in the case of ambiguous queries, "Request unclear" are generated. For backward compatibility, we design an Adapter to map functions/parameters to legacy domain-intent-slot structures.

**Judge** The traditional evaluation scheme for ICSF relies on the test set that requires full alignment of Intent and Slots. However, in real-world scenarios, there exist multiple solutions for function and slot selection. For example: (1) "Slightly increase the volume" could be resolved using either volume setting or volume increasing APIs; (2) "11:00 pm" and "23:00" semantically represent the same time. Additionally, due to crowdsourced annotators' limited understanding of specific business logic, the manual labeling accuracy remains suboptimal. As shown in [Figure 2c](#), the crowdsourced labeler's annotation accuracy has become the system bottleneck.

To address issues above, we introduce LLM-as-a-judge to evaluate prototype accuracy. We design a Judge based on QwQ-32B[44]: Given context and a set of Function & parameters, the Judge determines whether this combination semantically satisfies the user query. Following Samuylova's best practices<sup>1</sup>, we optimize the Judge using a 1k-expert-annotated dataset. Subsequently, both the LLM and 9 domain experts evaluate 3k test samples under identical conditions. Results show that Judge can provide logically coherent Chain-of-Thought(CoT) rationales and it achieves 93% consistency with expert judgments. Based on these findings, we conclude that LLM-as-a-Judge is the optimal evaluation approach for this task. As demonstrated in [Figure 4](#), we reconstruct the dialogue pipeline from BERT-based DC-ICSF architecture to LLM-based Function Call architecture. Evaluation through LLM-as-a-Judge demonstrates that the new architecture improves accuracy from 81.43% to 94.74% compared to the original one.

<sup>1</sup><https://www.evidentlyai.com/llm-guide/llm-as-a-judge>

### 3.2 Knowledge Transfer

**Rejection sampling Fine-Tuning** Building on our agent-oriented large model design, we propose Supervised Fine-Tuning (SFT) on smaller models using large model-generated data instead of relying solely on in-context learning (ICL) with large models. This approach offers two key benefits: (1) Smaller models can achieve performance comparable to large models after trained on sufficient high-quality data; (2) It significantly boosts inference and optimization efficiency. For a dataset  $D$  containing prompt component  $x$  and response component  $y$ , we define  $D(x, y) = \{x_i, y_i\}_{i=1}^N$ , where  $N$  denotes the dataset size. To minimize the Cross Entropy (CE) loss, we first utilize the SFT optimization, and then employ further optimization Rejection sampling Fine-Tuning (RFT). We use LLM judge introduced in [Section 3.1](#) to evaluate training data generated by the LLM prototype, filter out low-quality data, and generate the final training set. The actual training data is formulated as:

$$D_{filter} = \{x_i, y_i | \text{judge\_data}(x_i, y_i) = 1\}_{i=1}^N \quad (1)$$

where

$$\text{judge\_data}(x, y) = \begin{cases} 1, & \text{if the LLM judge thinks } y \text{ is a good answer for } x \\ 0, & \text{otherwise} \end{cases} \quad (2)$$

**Reinforcement Learning** Since OpenAI introduced Reinforcement Learning from Human Feedback (RLHF) [65], it has become an essential component for aligning LLMs, as evidenced in major technical reports [66; 67; 68; 11; 69]. DeepSeek-RL [43] proposes a cost-effective RL training method from scratch which combined rule-based ORM and GRPO [47]. Subsequent works like Logic-RL [8; 9; 10] applies this efficient approach across various tasks, enabling the model to automatically generate Chain of Thought (CoT) during training, thereby enhancing performance [70]. Based on our observation that model generalization degrades after RFT, we attempt to employ RL to improve model performance on out-of-domain datasets. Following Logic-RL [9], we refine the reward design for our specific task (see [Appendix B](#)) and conduct extensive attempts to integrate knowledge distillation (see [Appendix K](#)).

**Distillation** Using the Function Call-related data from large models and the RFT methods, we transfer capabilities from large to small models through training. To accelerate model training and inference, we implement prompt compression during training by removing unnecessary content from input-output pairs, including format specifications in inputs and Chain-of-Thought (CoT) rationales in outputs. Please refer to [Appendix C](#) for details.

Knowledge distillation [19] is an effective method for transferring knowledge from large to small models, requiring fewer data and exhibiting lower overfitting risks compared to SFT. We adopt the logits-based Adaptive Kullback-Leibler (AKL) distillation [29], with the optimization objective:

$$L_{AKL} = \mathbb{E}_{(x,y) \sim D} [AKL(\pi_\phi(y|x), \pi_\theta(y|x))] \quad (3)$$

$$AKL(p, q) = \alpha_{head} KL(p, q) + (1 - \alpha_{head}) KL(q, p) \quad (4)$$

$$KL(p, q) = \sum_k p_i \log \frac{p_i}{q_i} \quad (5)$$

where  $\pi_\theta$  denotes the trainable student model,  $\pi_\phi$  represents the teacher model, and  $\alpha_{head}$  is the head ratio in AKL. Setting  $\alpha_{head} = 1$  yields Forward KL Divergence-based distillation [25], while  $\alpha_{head} = 0$  corresponds to Reverse KL Divergence-based distillation [21].

We make optimizations on original methods: (1) Teacher Calibration: Following [71], we calibrate the teacher model with task-specific data to achieve lower student model loss; (2) Logits Pre-storage: For reducing training time, we pre-store teacher logits to enable multi-student distillation from a single cached logits set; (3) Top-k Pruning: We trim low-probability logits through top-k pruning, mitigating storage pressure and accelerating training speed.

### 3.3 Model Compression

**Pruning** To further compress model, we design two phases of pruning following NVIDIA [71], Llama3.2 [72], and Apple [73]: (1) Offline One-Shot Struct Pruning: Following Minitron[31], we explore two pruning strategies. For Depth Pruning, we compute layer importance scores and remove the  $N$  least important layers based on the target pruning ratio. For Width Pruning, we conduct a model architecture search using PPL-based criteria and prune channels according to group-wise importance rankings, with full implementation details in Section 1.1; (2) Recovery training: The first step is General Instruction Fine-tuning via Knowledge Distillation. Adopting Minitron’s approach, we leverage logits from a larger general instruction teacher model for recovery training. Due to unavailability of the teacher’s original training data, we first perform model correction on our selected IFT dataset to stabilize distillation, followed by top-k logits distillation(Section 3.2). The second step is Domain-Specific Task Alignment. The pruned compact LM undergoes further aligning through knowledge distillation, producing a final domain-optimized LLM.

**Quantization** Quantization typically reduces GPU memory consumption and enhances inference performance. In this work, we apply post-training quantization to smaller models obtained through distillation/pruning. Specifically, we implement two quantization approaches: 4-bit weight-only GPTQ algorithm [33] and full 8-bit weight-activation FP8 quantization [41]. The 4-bit weight-only quantization [33] compresses linear weights from FP16 to per-group INT4 via integer quantization, which are dequantized to FP16 during computation. This approach achieves notable inference acceleration in memory-bound scenarios with large model parameters and low GPU memory bandwidth. The FP8 quantization [41] quantizes both weights and activations to 8-bit floating-point format. Compared to 8-bit integer quantization [41], FP8 shows a more noticeable improvement in accuracy, and by utilizing NVIDIA’s FP8 tensor cores, FP8 can achieve effective inference acceleration [74].

## 4 Experiments

### 4.1 Experimental Setup

**Datasets** In our experiments, we utilize a large-scale dataset built from years of team experience and practice accumulated in the field. We reconstruct the intent classification and semantic slot framework within the real-world system into an API document specification, creating a function pool comprising 74 functional modules and 225 parameters. We sample 200k data points from a single business scenario as the training set and synthesize labels based on the LLM prototype outlined in Section 3.1. A combination of stratified and random sampling yields 11,922 samples from this scenario’s data as the in-domain test set. Additionally, we sample 7,867 data points using the same methodology from another business scenario, without some callable functions in the training set, as the out-of-domain test set. Compared to open-source datasets, our self-constructed dataset is more complex and closely aligned with real-world scenarios (see Table 1).

**Metrics** In accordance with the LLM-based Judge outlined in Section 3.1, we establish our evaluation metrics. Consider a dataset of size  $N$ , denoted as  $D(x, y) = \{x_i, y_i\}_{i=1}^N$ , where  $x$  signifies the prompt, including elements such as user queries, function lists, and dialogue histories, while  $y$  represents the response containing the function and its parameters. The function judge\_data, as rigorously defined in Equation 2, assesses whether the function and its parameter list can fulfill the specified user query. We define the Achievable Rate (AR) as follows:

$$\text{Achievable Rate (AR)} = \frac{1}{N} \sum_{i=1}^N \text{judge\_data}(x_i, y_i) \quad (6)$$

**Training** During the training phases, base models are all from small instruct models (0.5B-7B) of the Qwen2.5 model family [11]. We conduct RFT on them and RL on 7B models. We perform pruning on 0.5B models and obtain Qwen2.5-0.4B-Width and Qwen2.5-0.4B-Depth, both under a 20% pruning ratio. Then, we transfer knowledge from 7B RFT-trained models to pruned and 0.5B models via KD. We also apply KD from 7B RL-trained models to 0.5B models, followed by another RL phase (denoted as KD+RL). Finally, we use model quantization via W8A16/W4A16/W8A8



strategies on the KD-trained 0.5B model, detailed in [Appendix E](#). The training process is cost-efficient, utilizing only 8 NVIDIA H20 GPUs. Computing resources are listed in [Appendix F](#).

**Evaluation settings** We do evaluation by comparing our models with crowdsourced labelers and the BERT-based system consisting of two models based on BERT-large (330M)[75]. To evaluate the effectiveness of our method, we invite expert annotators alongside the LLM-as-a-judge-based metric AR (see [Equation 6](#)) for performance assessment. We also implement a retrieval module to select top 10 functions from the function pool, aiming to accelerate both training and inference phases, as detailed in [Appendix D](#). In real-world scenarios, we deploy models on NVIDIA L20 GPU and perform effectiveness evaluation via TensorRT-LLM[74], with specific configuration details provided in [Appendix H](#). During the comparison between the trained models and the BERT-based system, we adopt queries per second (QPS) as the primary metric for system throughput, response time (RT) for end-to-end latency, and concurrent clients (CC) to quantify high-concurrency performance.

## 4.2 Experimental Results

Table 2: Main results of the models trained on Qwen2.5(See [Appendix J](#) for FLOPs analysis).

Model / System	AR	GFLOPs
Crowdsourced Labelers	77.85%	-
BERT-based System	81.43%	38.65
Qwen2.5-72B (ICL)	94.74%	4907.50
Qwen2.5-7B (RFT)	95.29%	434.04
Qwen2.5-3B (RFT)	<b>95.30%</b>	218.94
Qwen2.5-1.5B (RFT)	95.16%	111.91
Qwen2.5-0.5B (RFT)	94.66%	43.31
Qwen2.5-0.5B (KD)	94.85%	43.31
Qwen2.5-0.5B-W8A16 (KD)	94.76%	-
Qwen2.5-0.5B-W4A16 (KD)	94.19%	-
Qwen2.5-0.5B-W8A8 (KD)	94.83%	-
Qwen2.5-0.4B-Width (KD)	94.17%	33.10
Qwen2.5-0.4B-Depth (KD)	94.20%	40.83

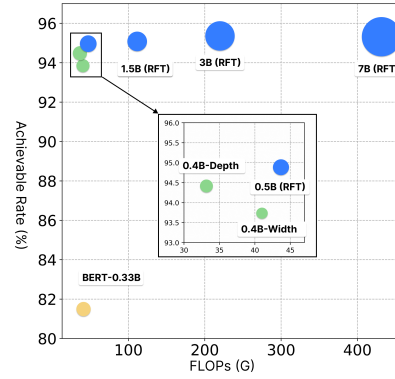


Figure 3: Cost and performance results. FLOPs reduced by 10x with nearly lossless AR.

Table 3: RFT vs RL on in-domain data and out-domain data.

Model	AR (ID)	AR (OOD)
Qwen2.5-72B (ICL)	94.74%	94.63%
Qwen2.5-7B (RFT)	95.29%	90.86%
Qwen2.5-0.5B (RFT)	94.66%	90.62%
Qwen2.5-7B (RL)	95.36%	<b>94.80%</b>
Qwen2.5-0.5B (KD*+RL)	<b>95.55%</b>	91.68%

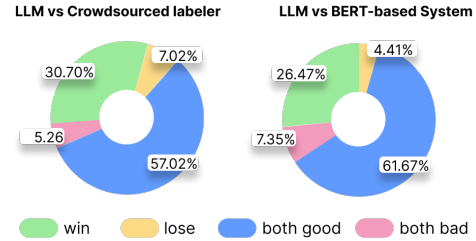


Figure 4: Comparison over different models by professional annotators

**LLM Prototype Preferred by Both Human and LLM-as-a-Judge** As illustrated in [Figure 4](#), annotations provided by professional annotators reveal that the LLM prototype (72B ICL) achieves a win+tie rate of 95.59% over the BERT-based system and 92.98% over crowdsourced labelers. This demonstrates the superior performance of the LLM prototype. Through the evaluation via LLM-as-a-Judge, we find that the LLM Prototype surpasses the BERT-based System by 13.31% and crowdsourced annotations by 16.89%, as shown in [Table 2](#). This conclusion is nearly consistent with that presented by professional annotators, demonstrating the effectiveness of the LLM judge.

**RFT and KD as Effective Knowledge Transfer Methods** As demonstrated in [Table 2](#), models trained with RFT generally exhibit a higher AR than the LLM prototype. Specifically, both the 3B and 7B models display negligible differences in performance and both achieves a 0.5% improvement

Table 4: Inference Performance under different model compression techniques.

Model	QPS					
	cc=1	cc=8	cc=16	cc=32	cc=64	cc=128
Qwen2.5-0.5B	39.11	166.71	248.62	348.87	459.12	517.13
Qwen2.5-0.5B-W8A16	44.11	169.86	251.21	346.17	445.84	521.41
Qwen2.5-0.5B-W4A16	<b>49.83</b>	<b>175.29</b>	256.05	338.16	453.46	519.22
Qwen2.5-0.5B-W8A8	40.40	158.15	<b>256.32</b>	<b>382.13</b>	<b>558.53</b>	<b>668.35</b>
Qwen2.5-0.4B-Width	43.65	167.65	260.58	372.59	502.82	581.23
Qwen2.5-0.4B-Depth	<b>45.22</b>	<b>198.82</b>	<b>309.62</b>	<b>438.58</b>	<b>566.87</b>	<b>650.26</b>
Qwen2.5-7B	4.43	14.77	17.71	19.04	19.79	20.06

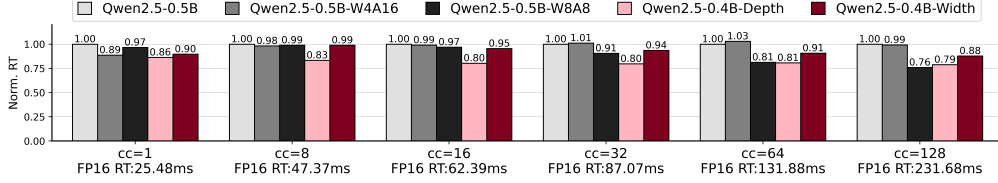


Figure 5: Normalized RT ratio based on FP16 models

in AR compared to the LLM prototype. The 0.5B model’s AR is 0.5% lower than the 1.5B model, while KD emerges as a valuable complement to RFT, enhancing the performance of the 0.5B model by an additional 0.19%. In terms of inference performance, the 0.5B model demonstrates only a slight 0.4% difference in AR compared to the 7B model, while achieving a significant 13.57x improvement in QPS and a substantial 91.3% reduction in latency, as illustrated in Table 4.

**RL’s Superior Generalization Ability** According to Table 3, while RFT performs well on in-domain data, it demonstrates worse results on out-of-domain data with a 3.61% AR decrease compared to the LLM prototype. Conversely, 7B RL-trained models achieve superior performance compared to other models on both in-domain and out-of-domain datasets, indicating better generalization of RL training methodology. Notably, even with models as small as 0.5B, employing a hybrid training methodology with KD+RL can yield superior in-domain results and an improvement of 1% in out-of-domain datasets compared to the RFT method. For more detailed exploration of the RL results, please refer to Appendix K.

**Tiny LLMs as a Cost-Efficient Upgrade to BERT-based System** As shown in Table 2 and Table 4, quantization minimally impacts accuracy, with less than a 0.1% AR loss, while significantly enhancing inference performance, achieving up to 1.29x higher QPS and 0.76x lower RT in the optimal scenario. Pruning incurs a slightly higher 0.2% accuracy loss but consistently enhances performance by 20%. For end-to-end inference, with a CC of 64, the BERT-based system reaches 1110.88 QPS and 55.84 ms RT. Although the cost is roughly twice that of the BERT-based system, the AR improves by up to absolute 14%.

## 5 Analysis

**Performance-Efficiency Trade-offs in Model Scaling** Our experimental analysis highlights a compelling trade-off between model size and computational efficiency. Although larger models typically show superior performance, the expected disparity between large and small ones is not as pronounced as anticipated. As shown in Figure 3, the 0.4B model achieves performance almost on par with the 7B model, efficiently requiring 11.8% FLOPs and reaching more than 17.4x QPS improvement and 92.9% RT reduction, with the 7B model’s RT being 882.552 ms under 16 CC. Although this model has a slight gap in cost compared to traditional BERT models, the improved accuracy and scalability stemming from LLM base makes it a favorable choice for various applications.

**Characteristics of Training Paradigms** The results presented in Table 3 underscore the distinct characteristics of different training methodologies. Fine-tuning primarily focuses on memorizing



data, making it susceptible to overfitting to the training set. In contrast, RL presents greater robustness by not merely fitting individual data points. We posit that RL’s superior generalization capabilities stem from its ability to learn from negative samples, which are generated by the model being trained itself. RL is highly effective for dealing with well-structured problems, while it has unsatisfactory convergence facing ambiguous data or a lack of domain knowledge in real-world tasks. Additionally, applying RL directly to tiny models often proves to be ineffective, likely due to such models’ limited capacity to utilize Chain-of-Thought (CoT) rationales. In such cases, KD can compensate for this limitation by training the tiny models on a large amount of CoT data generated by a RL-trained teacher model. Compared to fine-tuning, KD can better extract CoT rationales from the probability distribution. Consequently, the hybrid methodology of KD and RL can achieve remarkably enhanced performance and represents a promising direction for future development.

**Comparison over Model Compression Strategies** Our analysis identifies depth pruning as the optimal approach for domain-specific models. Depth pruning achieves 20% inference acceleration with lossless AR at same compression ratios (Table 2), stemming from the nature of depth pruning, removing entire transformer layers and their associated attention computations. Although width pruning exhibits slightly better effects in general instruction tasks after training (Table 9), depth pruning presents optimal efficiency facing long prompts, with width pruning focusing on matrix optimizations (Appendix J). Regarding quantization, the W4A16 strategy achieves impressive performance in single-thread scenarios, while FP8 outperforms with lossless accuracy under high concurrency conditions as the superior paradigm for throughput deployments.

## 6 Conclusion

Based on our comprehensive study, several key insights emerge regarding the development and deployment of effective deep learning models in practical scenarios.

**Tiny Models as a Practical Low-Cost Alternative** Our experiments indicate that end-to-end optimized tiny models can achieve performance levels comparable to their larger counterparts, offering resource efficiency without compromising accuracy. This provides an alternative pathway for applying LLMs in practical tasks under low-cost scenarios.

**Balanced Focus Beyond AGI** While AGI remains a visionary long-term aim for LLMs, progress has reached a plateau, prompting increased attention towards real-world applicability. Our work demonstrates that integrating LLM-driven techniques into traditional tasks results in immediate, measurable improvements. It advocates for a balanced research agenda that equally emphasizes foundational advancements and domain-specific applications.

**Scalable Cost-Efficient Three-Stage Pipeline** The proposed pipeline-comprising prototyping, knowledge transfer, and model compression-presents a systematic framework designed to achieve high performance while maintaining low costs in both training and inference. We believe that this approach can be effectively adapted to other domains, thereby potentially advancing research in those areas and facilitating the widespread deployment of LLMs.

## 7 Limitation & Future Works

Our pipeline has presented optimal cost-performance results, and our super tiny models have exhibited remarkable capabilities, featuring low latency, cost efficiency, cloud independence, and robust privacy. Further compression may offer limited marginal benefits. Thus, we are more focused on enhancing such models’ capabilities and expand their broader applications such as mobile devices:

**Hybrid Methodology for LLMs Capabilities Transfer** Based on our existing experiments, the mixer of reinforcement learning and knowledge distillation has effectively enhanced the generalization capabilities of super tiny models. This implies a potentially powerful hybrid methodology that allows super tiny models to nearly fully retain the capabilities of LLMs in domain-specific tasks. In future research, we will build upon our previous work to conduct deeper studies and theoretical analyses of this hybrid approach in transferring LLMs capabilities to such super tiny models.

**On-device Deployment Optimization** Although we achieve 8-bit compression and online deployment, real-world edge devices face heterogeneous hardware constraints such as memory fragmentation and NPU compatibility. In the future, for on-device deployment of super tiny models, we will develop hardware-aware compression algorithms and adaptive runtime kernels to optimize latency-energy tradeoffs across diverse IoT ecosystems, and explore more resource-efficient deployment techniques for edge devices, such as sparse computation, edge-centric quantization, and federated learning.

## References

- [1] Meng-Hao Guo, Zheng-Ning Liu, Tai-Jiang Mu, and Shi-Min Hu. Beyond self-attention: External attention using two linear layers for visual tasks, 2021.
- [2] Romal Thoppilan, Daniel De Freitas, Jamie Hall, Noam Shazeer, Apoorv Kulshreshtha, Heng-Tze Cheng, Alicia Jin, Taylor Bos, Leslie Baker, Yu Du, YaGuang Li, Hongrae Lee, Huaixiu Steven Zheng, Amin Ghafouri, Marcelo Menegali, Yanping Huang, Maxim Krikun, Dmitry Lepikhin, James Qin, Dehao Chen, Yuanzhong Xu, Zhifeng Chen, Adam Roberts, Maarten Bosma, Vincent Zhao, Yanqi Zhou, Chung-Ching Chang, Igor Krivokon, Will Rusch, Marc Pickett, Pranesh Srinivasan, Laichee Man, Kathleen Meier-Hellstern, Meredith Ringel Morris, Tulsee Doshi, Renelito Delos Santos, Toju Duke, Johnny Soraker, Ben Zevenbergen, Vinodkumar Prabhakaran, Mark Diaz, Ben Hutchinson, Kristen Olson, Alejandra Molina, Erin Hoffman-John, Josh Lee, Lora Aroyo, Ravi Rajakumar, Alena Butryna, Matthew Lamm, Viktoriya Kuzmina, Joe Fenton, Aaron Cohen, Rachel Bernstein, Ray Kurzweil, Blaise Aguerre-Arcas, Claire Cui, Marian Croak, Ed Chi, and Quoc Le. Lamda: Language models for dialog applications, 2022.
- [3] Alan Akbik, Duncan Blythe, and Roland Vollgraf. Contextual string embeddings for sequence labeling. In Emily M. Bender, Leon Derczynski, and Pierre Isabelle, editors, *Proceedings of the 27th International Conference on Computational Linguistics*, pages 1638–1649, Santa Fe, New Mexico, USA, August 2018. Association for Computational Linguistics.
- [4] Deepak Narayanan, Mohammad Shoeybi, Jared Casper, Patrick LeGresley, Mostofa Patwary, Vijay Anand Korthikanti, Dmitri Vainbrand, Prethvi Kashinkunti, Julie Bernauer, Bryan Catanzaro, Amar Phanishayee, and Matei Zaharia. Efficient large-scale language model training on gpu clusters using megatron-lm, 2021.
- [5] Mo Zhao, Ya Ma, Zhendong Li, and Hao Liu. Cross-dataset pose estimation of faces in the wild. In *2021 5th Asian Conference on Artificial Intelligence Technology (ACAIT)*, pages 718–724, 2021.
- [6] Julia Gusak, Daria Cherniuk, Alena Shilova, Alexander Katrutsa, Daniel Bershatsky, Xunyi Zhao, Lionel Eyraud-Dubois, Oleg Shlyazhko, Denis Dimitrov, Ivan Oseledets, and Olivier Beaumont. Survey on large scale neural network training, 2022.
- [7] Yan Li, So-Eon Kim, Seong-Bae Park, and Soyeon Caren Han. Midas: Multi-level intent, domain, and slot knowledge distillation for multi-turn nlu, 2025.
- [8] Jingcheng Hu, Yinmin Zhang, Qi Han, Daxin Jiang, and Heung-Yeung Shum Xiangyu Zhang. Open-reasoner-zero: An open source approach to scaling reinforcement learning on the base model. <https://github.com/Open-Reasoner-Zero/Open-Reasoner-Zero>, 2025.
- [9] Tian Xie, Zitian Gao, Qingnan Ren, Haoming Luo, Yuqian Hong, Bryan Dai, Joey Zhou, Kai Qiu, Zhirong Wu, and Chong Luo. Logic-rl: Unleashing llm reasoning with rule-based reinforcement learning, 2025.
- [10] Jiayi Pan, Junjie Zhang, Xingyao Wang, Lifan Yuan, Hao Peng, and Alane Suhr. Tinyzero. <https://github.com/Jiayi-Pan/TinyZero>, 2025. Accessed: 2025-01-24.
- [11] Qwen, :, An Yang, Baosong Yang, Beichen Zhang, Binyuan Hui, Bo Zheng, Bowen Yu, Chengyuan Li, Dayiheng Liu, Fei Huang, Haoran Wei, Huan Lin, Jian Yang, Jianhong Tu, Jianwei Zhang, Jianxin Yang, Jiaxi Yang, Jingren Zhou, Junyang Lin, Kai Dang, Keming Lu, Keqin Bao, Kexin Yang, Le Yu, Mei Li, Mingfeng Xue, Pei Zhang, Qin Zhu, Rui Men, Runji Lin, Tianhao Li, Tianyi Tang, Tingyu Xia, Xingzhang Ren, Xuancheng Ren, Yang Fan, Yang

- Su, Yichang Zhang, Yu Wan, Yuqiong Liu, Zeyu Cui, Zhenru Zhang, and Zihan Qiu. Qwen2.5 technical report, 2025.
- [12] Timo Schick, Jane Dwivedi-Yu, Roberto Dessì, Roberta Raileanu, Maria Lomeli, Eric Hambro, Luke Zettlemoyer, Nicola Cancedda, and Thomas Scialom. Toolformer: Language models can teach themselves to use tools. In Alice Oh, Tristan Naumann, Amir Globerson, Kate Saenko, Moritz Hardt, and Sergey Levine, editors, *Advances in Neural Information Processing Systems 36: Annual Conference on Neural Information Processing Systems 2023, NeurIPS 2023, New Orleans, LA, USA, December 10 - 16, 2023*, 2023.
  - [13] Shishir G. Patil, Tianjun Zhang, Xin Wang, and Joseph E. Gonzalez. Gorilla: Large language model connected with massive apis. In Amir Globersons, Lester Mackey, Danielle Belgrave, Angela Fan, Ulrich Paquet, Jakub M. Tomczak, and Cheng Zhang, editors, *Advances in Neural Information Processing Systems 38: Annual Conference on Neural Information Processing Systems 2024, NeurIPS 2024, Vancouver, BC, Canada, December 10 - 15, 2024*, 2024.
  - [14] Lutfi Eren Erdogan, Nicholas Lee, Siddharth Jha, Sehoon Kim, Ryan Tabrizi, Suhong Moon, Coleman Hooper, Gopala Anumanchipalli, Kurt Keutzer, and Amir Gholami. Tinyagent: Function calling at the edge, 2024.
  - [15] Mohammad Kachuee, Sarthak Ahuja, Vaibhav Kumar, Puyang Xu, and Xiaohu Liu. Improving tool retrieval by leveraging large language models for query generation, 2024.
  - [16] Tom Kocmi and Christian Federmann. Large language models are state-of-the-art evaluators of translation quality. In Mary Nurminen, Judith Brenner, Maarit Koponen, Sirkku Lomaa, Mikhail Mikhailov, Frederike Schierl, Tharindu Ranasinghe, Eva Vanmassenhove, Sergi Alvarez Vidal, Nora Aranberri, Mara Nunziatini, Carla Parra Escartín, Mikel L. Forcada, Maja Popovic, Carolina Scarton, and Helena Moniz, editors, *Proceedings of the 24th Annual Conference of the European Association for Machine Translation, EAMT 2023, Tampere, Finland, 12-15 June 2023*, pages 193–203. European Association for Machine Translation, 2023.
  - [17] Lianmin Zheng, Wei-Lin Chiang, Ying Sheng, Siyuan Zhuang, Zhanghao Wu, Yonghao Zhuang, Zi Lin, Zhuohan Li, Dacheng Li, Eric P. Xing, Hao Zhang, Joseph E. Gonzalez, and Ion Stoica. Judging llm-as-a-judge with mt-bench and chatbot arena. In Alice Oh, Tristan Naumann, Amir Globerson, Kate Saenko, Moritz Hardt, and Sergey Levine, editors, *Advances in Neural Information Processing Systems 36: Annual Conference on Neural Information Processing Systems 2023, NeurIPS 2023, New Orleans, LA, USA, December 10 - 16, 2023*, 2023.
  - [18] Nat McAleese, Rai Michael Pokorny, Juan Felipe Ceron Uribe, Evgenia Nitishinskaya, Maja Trebacz, and Jan Leike. Llm critics help catch llm bugs, 2024.
  - [19] Geoffrey E. Hinton, Oriol Vinyals, and Jeffrey Dean. Distilling the knowledge in a neural network. *CoRR*, abs/1503.02531, 2015.
  - [20] Yuxian Gu, Li Dong, Furu Wei, and Minlie Huang. Minillm: Knowledge distillation of large language models. In *The Twelfth International Conference on Learning Representations, ICLR 2024, Vienna, Austria, May 7-11, 2024*. OpenReview.net, 2024.
  - [21] Yixing Li, Yuxian Gu, Li Dong, Dequan Wang, Yu Cheng, and Furu Wei. Direct preference knowledge distillation for large language models. *arXiv preprint arXiv:2406.19774*, 2024.
  - [22] Chuanguang Yang, Xinqiang Yu, Zhulin An, and Yongjun Xu. Categories of response-based, feature-based, and relation-based knowledge distillation, 2023.
  - [23] Yoon Kim and Alexander M. Rush. Sequence-level knowledge distillation. In Jian Su, Xavier Carreras, and Kevin Duh, editors, *Proceedings of the 2016 Conference on Empirical Methods in Natural Language Processing, EMNLP 2016, Austin, Texas, USA, November 1-4, 2016*, pages 1317–1327. The Association for Computational Linguistics, 2016.
  - [24] Minsoo Kim, Sihwa Lee, Janghwan Lee, Sukjin Hong, Du-Seong Chang, Wonyong Sung, and Jungwook Choi. Token-scaled logit distillation for ternary weight generative language models, 2023.

- [25] Victor Sanh, Lysandre Debut, Julien Chaumond, and Thomas Wolf. Distilbert, a distilled version of bert: smaller, faster, cheaper and lighter, 2020.
- [26] Yuxian Gu, Li Dong, Furu Wei, and Minlie Huang. Minillm: Knowledge distillation of large language models, 2024.
- [27] Rishabh Agarwal, Nino Vieillard, Yongchao Zhou, Piotr Stanczyk, Sabela Ramos, Matthieu Geist, and Olivier Bachem. On-policy distillation of language models: Learning from self-generated mistakes, 2024.
- [28] Gyeongman Kim, Doohyuk Jang, and Eunho Yang. Promptkd: Distilling student-friendly knowledge for generative language models via prompt tuning, 2024.
- [29] Taiqiang Wu, Chaofan Tao, Jiahao Wang, Runming Yang, Zhe Zhao, and Ngai Wong. Rethinking kullback-leibler divergence in knowledge distillation for large language models. In Owen Rambow, Leo Wanner, Marianna Apidianaki, Hend Al-Khalifa, Barbara Di Eugenio, and Steven Schockaert, editors, *Proceedings of the 31st International Conference on Computational Linguistics, COLING 2025, Abu Dhabi, UAE, January 19-24, 2025*, pages 5737–5755. Association for Computational Linguistics, 2025.
- [30] Elias Frantar and Dan Alistarh. Sparsegpt: Massive language models can be accurately pruned in one-shot, 2023.
- [31] Xinyin Ma, Gongfan Fang, and Xinchao Wang. Llm-pruner: On the structural pruning of large language models, 2023.
- [32] Tim Dettmers, Mike Lewis, Younes Belkada, and Luke Zettlemoyer. Llm.int8(): 8-bit matrix multiplication for transformers at scale, 2022.
- [33] Elias Frantar, Saleh Ashkboos, Torsten Hoefer, and Dan Alistarh. Gptq: Accurate post-training quantization for generative pre-trained transformers, 2023.
- [34] Guangxuan Xiao, Ji Lin, Mickael Seznec, Hao Wu, Julien Demouth, and Song Han. Smoothquant: Accurate and efficient post-training quantization for large language models, 2024.
- [35] Hao Li, Asim Kadav, Igor Durdanovic, Hanan Samet, and Hans Peter Graf. Pruning filters for efficient convnets, 2017.
- [36] Xin Men, Mingyu Xu, Qingyu Zhang, Bingning Wang, Hongyu Lin, Yaojie Lu, Xianpei Han, and Weipeng Chen. Shortgpt: Layers in large language models are more redundant than you expect, 2024.
- [37] Saurav Muralidharan, Sharath Turuvekere Sreenivas, Raviraj Joshi, Marcin Chochowski, Mostofa Patwary, Mohammad Shoeybi, Bryan Catanzaro, Jan Kautz, and Pavlo Molchanov. Compact language models via pruning and knowledge distillation, 2024.
- [38] Mengzhou Xia, Tianyu Gao, Zhiyuan Zeng, and Danqi Chen. Sheared llama: Accelerating language model pre-training via structured pruning, 2024.
- [39] Song Guo, Jiahang Xu, Li Lyna Zhang, and Mao Yang. Compresso: Structured pruning with collaborative prompting learns compact large language models, 2023.
- [40] Ji Lin, Jiaming Tang, Haotian Tang, Shang Yang, Wei-Ming Chen, Wei-Chen Wang, Guangxuan Xiao, Xingyu Dang, Chuang Gan, and Song Han. Awq: Activation-aware weight quantization for llm compression and acceleration, 2024.
- [41] Andrey Kuzmin, Mart Van Baalen, Yuwei Ren, Markus Nagel, Jorn Peters, and Tijmen Blankevoort. Fp8 quantization: The power of the exponent, 2024.
- [42] Yujun Lin, Haotian Tang, Shang Yang, Zhekai Zhang, Guangxuan Xiao, Chuang Gan, and Song Han. Qserve: W4a8kv4 quantization and system co-design for efficient llm serving, 2024.

- [43] DeepSeek-AI, Daya Guo, Dejian Yang, Haowei Zhang, Junxiao Song, Ruoyu Zhang, Runxin Xu, Qihao Zhu, Shirong Ma, Peiyi Wang, Xiao Bi, Xiaokang Zhang, Xingkai Yu, Yu Wu, Z. F. Wu, Zhibin Gou, Zhihong Shao, Zhuoshu Li, Ziyi Gao, Aixin Liu, Bing Xue, Bingxuan Wang, Bochao Wu, Bei Feng, Chengda Lu, Chenggang Zhao, Chengqi Deng, Chenyu Zhang, Chong Ruan, Damai Dai, Deli Chen, Dongjie Ji, Erhang Li, Fangyun Lin, Fucong Dai, Fuli Luo, Guangbo Hao, Guanting Chen, Guowei Li, H. Zhang, Han Bao, Hanwei Xu, Haocheng Wang, Honghui Ding, Huajian Xin, Huazuo Gao, Hui Qu, Hui Li, Jianzhong Guo, Jiashi Li, Jiawei Wang, Jingchang Chen, Jingyang Yuan, Junjie Qiu, Junlong Li, J. L. Cai, Jiaqi Ni, Jian Liang, Jin Chen, Kai Dong, Kai Hu, Kaige Gao, Kang Guan, Kexin Huang, Kuai Yu, Lean Wang, Lecong Zhang, Liang Zhao, Litong Wang, Liyue Zhang, Lei Xu, Leyi Xia, Mingchuan Zhang, Minghua Zhang, Minghui Tang, Meng Li, Miaojun Wang, Mingming Li, Ning Tian, Panpan Huang, Peng Zhang, Qiancheng Wang, Qinyu Chen, Qiushi Du, Ruiqi Ge, Ruisong Zhang, Ruizhe Pan, Runji Wang, R. J. Chen, R. L. Jin, Ruyi Chen, Shanghao Lu, Shangyan Zhou, Shanhua Chen, Shengfeng Ye, Shiyu Wang, Shuiping Yu, Shunfeng Zhou, Shuting Pan, S. S. Li, Shuang Zhou, Shaoqing Wu, Shengfeng Ye, Tao Yun, Tian Pei, Tianyu Sun, T. Wang, Wangding Zeng, Wanbiao Zhao, Wen Liu, Wenfeng Liang, Wenjun Gao, Wenqin Yu, Wentao Zhang, W. L. Xiao, Wei An, Xiaodong Liu, Xiaohan Wang, Xiaokang Chen, Xiaotao Nie, Xin Cheng, Xin Liu, Xin Xie, Xingchao Liu, Xinyu Yang, Xinyuan Li, Xuecheng Su, Xuheng Lin, X. Q. Li, Xiangyue Jin, Xiaojin Shen, Xiaosha Chen, Xiaowen Sun, Xiaoxiang Wang, Xinnan Song, Xinyi Zhou, Xianzu Wang, Xinxia Shan, Y. K. Li, Y. Q. Wang, Y. X. Wei, Yang Zhang, Yanhong Xu, Yao Li, Yao Zhao, Yaofeng Sun, Yaohui Wang, Yi Yu, Yichao Zhang, Yifan Shi, Yiliang Xiong, Ying He, Yishi Piao, Yisong Wang, Yixuan Tan, Yiyang Ma, Yiyuan Liu, Yongqiang Guo, Yuan Ou, Yuduan Wang, Yue Gong, Yuheng Zou, Yujia He, Yunfan Xiong, Yuxiang Luo, Yuxiang You, Yuxuan Liu, Yuyang Zhou, Y. X. Zhu, Yanhong Xu, Yanping Huang, Yaohui Li, Yi Zheng, Yuchen Zhu, Yunxian Ma, Ying Tang, Yukun Zha, Yuting Yan, Z. Z. Ren, Zehui Ren, Zhangli Sha, Zhe Fu, Zhen Xu, Zhenda Xie, Zhengyan Zhang, Zhewen Hao, Zhicheng Ma, Zhigang Yan, Zhiyu Wu, Zihui Gu, Zijia Zhu, Zijun Liu, Zilin Li, Ziwei Xie, Ziyang Song, Zizheng Pan, Zhen Huang, Zhipeng Xu, Zhongyu Zhang, and Zhen Zhang. Deepseek-r1: Incentivizing reasoning capability in llms via reinforcement learning, 2025.
- [44] Qwen Team. Qwq-32b: Embracing the power of reinforcement learning, March 2025.
- [45] Aaron Jaech, Adam Kalai, Adam Lerer, Adam Richardson, Ahmed El-Kishky, Aiden Low, Alec Helyar, Aleksander Madry, Alex Beutel, Alex Carney, Alex Iftimie, Alex Karpenko, Alex Tachard Passos, Alexander Neitz, Alexander Prokofiev, Alexander Wei, Allison Tam, Ally Bennett, Ananya Kumar, Andre Saraiva, Andrea Vallone, Andrew Duberstein, Andrew Kondrich, Andrey Mishchenko, Andy Applebaum, Angela Jiang, Ashvin Nair, Barret Zoph, Behrooz Ghorbani, Ben Rossen, Benjamin Sokolowsky, Boaz Barak, Bob McGrew, Borys Minaiev, Botao Hao, Bowen Baker, Brandon Houghton, Brandon McKinzie, Brydon Eastman, Camillo Lugaresi, Cary Bassin, Cary Hudson, Chak Ming Li, Charles de Bourcy, Chelsea Voss, Chen Shen, Chong Zhang, Chris Koch, Chris Orsinger, Christopher Hesse, Claudia Fischer, Clive Chan, Dan Roberts, Daniel Kappler, Daniel Levy, Daniel Selsam, David Dohan, David Farhi, David Mely, David Robinson, Dimitris Tsipras, Doug Li, Dragos Oprica, Eben Freeman, Eddie Zhang, Edmund Wong, Elizabeth Proehl, Enoch Cheung, Eric Mitchell, Eric Wallace, Erik Ritter, Evan Mays, Fan Wang, Felipe Petroski Such, Filippo Raso, Florencia Leoni, Foivos Tsimpourlas, Francis Song, Fred von Lohmann, Freddie Sulit, Geoff Salmon, Giambattista Parascandolo, Gildas Chabot, Grace Zhao, Greg Brockman, Guillaume Leclerc, Hadi Salman, Haiming Bao, Hao Sheng, Hart Andrin, Hessam Bagherinezhad, Hongyu Ren, Hunter Lightman, Hyung Won Chung, Ian Kivlichan, Ian O’Connell, Ian Osband, Ignasi Clavera Gilaberte, and Ilge Akkaya. Openai o1 system card. *CoRR*, abs/2412.16720, 2024.
- [46] John Schulman, Filip Wolski, Prafulla Dhariwal, Alec Radford, and Oleg Klimov. Proximal policy optimization algorithms. *CoRR*, abs/1707.06347, 2017.
- [47] Zhihong Shao, Peiyi Wang, Qihao Zhu, Runxin Xu, Junxiao Song, Mingchuan Zhang, Y. K. Li, Y. Wu, and Daya Guo. Deepseekmath: Pushing the limits of mathematical reasoning in open language models. *CoRR*, abs/2402.03300, 2024.
- [48] Arash Ahmadian, Chris Cremer, Matthias Gallé, Marzieh Fadaee, Julia Kreutzer, Olivier Pietquin, Ahmet Üstün, and Sara Hooker. Back to basics: Revisiting reinforce-style optimiza-

- tion for learning from human feedback in llms. In Lun-Wei Ku, Andre Martins, and Vivek Srikumar, editors, *Proceedings of the 62nd Annual Meeting of the Association for Computational Linguistics (Volume 1: Long Papers)*, ACL 2024, Bangkok, Thailand, August 11-16, 2024, pages 12248–12267. Association for Computational Linguistics, 2024.
- [49] Ziniu Li, Tian Xu, Yushun Zhang, Zhihang Lin, Yang Yu, Ruoyu Sun, and Zhi-Quan Luo. Remax: A simple, effective, and efficient reinforcement learning method for aligning large language models. In *Forty-first International Conference on Machine Learning, ICML 2024, Vienna, Austria, July 21-27, 2024*. OpenReview.net, 2024.
  - [50] Jian Hu. Reinforce++: A simple and efficient approach for aligning large language models, 2025.
  - [51] Rafael Rafailov, Archit Sharma, Eric Mitchell, Christopher D. Manning, Stefano Ermon, and Chelsea Finn. Direct preference optimization: Your language model is secretly a reward model. In Alice Oh, Tristan Naumann, Amir Globerson, Kate Saenko, Moritz Hardt, and Sergey Levine, editors, *Advances in Neural Information Processing Systems 36: Annual Conference on Neural Information Processing Systems 2023, NeurIPS 2023, New Orleans, LA, USA, December 10 - 16, 2023*, 2023.
  - [52] Kawin Ethayarajh, Winnie Xu, Niklas Muennighoff, Dan Jurafsky, and Douwe Kiela. Model alignment as prospect theoretic optimization. In *Forty-first International Conference on Machine Learning, ICML 2024, Vienna, Austria, July 21-27, 2024*. OpenReview.net, 2024.
  - [53] Jiwoo Hong, Noah Lee, and James Thorne. ORPO: monolithic preference optimization without reference model. In Yaser Al-Onaizan, Mohit Bansal, and Yun-Nung Chen, editors, *Proceedings of the 2024 Conference on Empirical Methods in Natural Language Processing, EMNLP 2024, Miami, FL, USA, November 12-16, 2024*, pages 11170–11189. Association for Computational Linguistics, 2024.
  - [54] Yu Meng, Mengzhou Xia, and Danqi Chen. Simpo: Simple preference optimization with a reference-free reward. In Amir Globersons, Lester Mackey, Danielle Belgrave, Angela Fan, Ulrich Paquet, Jakub M. Tomczak, and Cheng Zhang, editors, *Advances in Neural Information Processing Systems 38: Annual Conference on Neural Information Processing Systems 2024, NeurIPS 2024, Vancouver, BC, Canada, December 10 - 15, 2024*, 2024.
  - [55] Zixiang Chen, Yihe Deng, Huizhuo Yuan, Kaixuan Ji, and Quanquan Gu. Self-play fine-tuning converts weak language models to strong language models. In *Forty-first International Conference on Machine Learning, ICML 2024, Vienna, Austria, July 21-27, 2024*. OpenReview.net, 2024.
  - [56] Eugene Choi, Arash Ahmadian, Matthieu Geist, Olivier Pietquin, and Mohammad Gheshlaghi Azar. Self-improving robust preference optimization. *CoRR*, abs/2406.01660, 2024.
  - [57] Zhenting Qi, Mingyuan Ma, Jiahang Xu, Li Lyna Zhang, Fan Yang, and Mao Yang. Mutual reasoning makes smaller llms stronger problem-solvers. *CoRR*, abs/2408.06195, 2024.
  - [58] Zhaohan Daniel Guo, Gökhan Tür, Wen-tau Yih, and Geoffrey Zweig. Joint semantic utterance classification and slot filling with recursive neural networks. In *2014 IEEE Spoken Language Technology Workshop, SLT 2014, South Lake Tahoe, NV, USA, December 7-10, 2014*, pages 554–559. IEEE, 2014.
  - [59] Alice Coucke, Alaa Saade, Adrien Ball, Théodore Bluche, Alexandre Caulier, David Leroy, Clément Doumouro, Thibault Gisselbrecht, Francesco Caltagirone, Thibaut Lavril, Maël Primet, and Joseph Dureau. Snips voice platform: an embedded spoken language understanding system for private-by-design voice interfaces. *CoRR*, abs/1805.10190, 2018.
  - [60] Qian Chen, Zhu Zhuo, and Wen Wang. Bert for joint intent classification and slot filling, 2019.
  - [61] Diogo Tavares, Pedro Azevedo, David Semedo, Ricardo Gamelas Sousa, and João Magalhães. Task conditioned BERT for joint intent detection and slot-filling. In Nuno Moniz, Zita Vale, José Cascalho, Catarina Silva, and Raquel Sebastião, editors, *Progress in Artificial Intelligence - 22nd EPIA Conference on Artificial Intelligence, EPIA 2023, Faial Island, Azores, September*



- 5-8, 2023, *Proceedings, Part I*, volume 14115 of *Lecture Notes in Computer Science*, pages 467–480. Springer, 2023.
- [62] Patrick Lewis, Ethan Perez, Aleksandra Piktus, Fabio Petroni, Vladimir Karpukhin, Naman Goyal, Heinrich Küttler, Mike Lewis, Wen tau Yih, Tim Rocktäschel, Sebastian Riedel, and Douwe Kiela. Retrieval-augmented generation for knowledge-intensive nlp tasks, 2021.
  - [63] Zehan Li, Xin Zhang, Yanzhao Zhang, Dingkun Long, Pengjun Xie, and Meishan Zhang. Towards general text embeddings with multi-stage contrastive learning. *arXiv preprint arXiv:2308.03281*, 2023.
  - [64] Jeff Johnson, Matthijs Douze, and Hervé Jégou. Billion-scale similarity search with GPUs. *IEEE Transactions on Big Data*, 7(3):535–547, 2019.
  - [65] Long Ouyang, Jeff Wu, Xu Jiang, Diogo Almeida, Carroll L. Wainwright, Pamela Mishkin, Chong Zhang, Sandhini Agarwal, Katarina Slama, Alex Ray, John Schulman, Jacob Hilton, Fraser Kelton, Luke Miller, Maddie Simens, Amanda Askell, Peter Welinder, Paul Christiano, Jan Leike, and Ryan Lowe. Training language models to follow instructions with human feedback, 2022.
  - [66] Hugo Touvron, Thibaut Lavril, Gautier Izacard, Xavier Martinet, Marie-Anne Lachaux, Timothée Lacroix, Baptiste Rozière, Naman Goyal, Eric Hambro, Faisal Azhar, Aurelien Rodriguez, Armand Joulin, Edouard Grave, and Guillaume Lample. Llama: Open and efficient foundation language models, 2023.
  - [67] Hugo Touvron, Louis Martin, Kevin Stone, Peter Albert, Amjad Almahairi, Yasmine Babaei, Nikolay Bashlykov, Soumya Batra, Prajjwal Bhargava, Shruti Bhosale, Dan Bikel, Lukas Blecher, Cristian Canton Ferrer, Moya Chen, Guillem Cucurull, David Esiobu, Jude Fernandes, Jeremy Fu, Wenyin Fu, Brian Fuller, Cynthia Gao, Vedanuj Goswami, Naman Goyal, Anthony Hartshorn, Saghar Hosseini, Rui Hou, Hakan Inan, Marcin Kardas, Viktor Kerkez, Madian Khabsa, Isabel Kloumann, Artem Korenev, Punit Singh Koura, Marie-Anne Lachaux, Thibaut Lavril, Jenya Lee, Diana Liskovich, Yinghai Lu, Yuning Mao, Xavier Martinet, Todor Mihaylov, Pushkar Mishra, Igor Molybog, Yixin Nie, Andrew Poulton, Jeremy Reizenstein, Rashi Rungta, Kalyan Saladi, Alan Schelten, Ruan Silva, Eric Michael Smith, Ranjan Subramanian, Xiaoqing Ellen Tan, Binh Tang, Ross Taylor, Adina Williams, Jian Xiang Kuan, Puxin Xu, Zheng Yan, Iliyan Zarov, Yuchen Zhang, Angela Fan, Melanie Kambadur, Sharan Narang, Aurelien Rodriguez, Robert Stojnic, Sergey Edunov, and Thomas Scialom. Llama 2: Open foundation and fine-tuned chat models, 2023.
  - [68] Jinze Bai, Shuai Bai, Yunfei Chu, Zeyu Cui, Kai Dang, Xiaodong Deng, Yang Fan, Wenbin Ge, Yu Han, Fei Huang, Binyuan Hui, Luo Ji, Mei Li, Junyang Lin, Runji Lin, Dayiheng Liu, Gao Liu, Chengqiang Lu, Keming Lu, Jianxin Ma, Rui Men, Xingzhang Ren, Xuancheng Ren, Chuanqi Tan, Sinan Tan, Jianhong Tu, Peng Wang, Shijie Wang, Wei Wang, Shengguang Wu, Benfeng Xu, Jin Xu, An Yang, Hao Yang, Jian Yang, Shusheng Yang, Yang Yao, Bowen Yu, Hongyi Yuan, Zheng Yuan, Jianwei Zhang, Xingxuan Zhang, Yichang Zhang, Zhenru Zhang, Chang Zhou, Jingren Zhou, Xiaohuan Zhou, and Tianhang Zhu. Qwen technical report, 2023.
  - [69] Gemma Team, Morgane Riviere, Shreya Pathak, Pier Giuseppe Sessa, Cassidy Hardin, Surya Bhupatiraju, Léonard Hussenot, Thomas Mesnard, Bobak Shahriari, Alexandre Ramé, Johan Ferret, Peter Liu, Pouya Tafti, Abe Friesen, Michelle Casbon, Sabela Ramos, Ravin Kumar, Charline Le Lan, Sammy Jerome, Anton Tsitsulin, Nino Vieillard, Piotr Stanczyk, Sertan Girgin, Nikola Momchev, Matt Hoffman, Shantanu Thakoor, Jean-Bastien Grill, Behnam Neyshabur, Olivier Bachem, Alanna Walton, Aliaksei Severyn, Alicia Parrish, Aliya Ahmad, Allen Hutchison, Alvin Abdagic, Amanda Carl, Amy Shen, Andy Brock, Andy Coenen, Anthony Laforge, Antonia Paterson, Ben Bastian, Bilal Piot, Bo Wu, Brandon Royal, Charlie Chen, Chintu Kumar, Chris Perry, Chris Welty, Christopher A. Choquette-Choo, Danila Sinopalnikov, David Weinberger, Dimple Vijaykumar, Dominika Rogozińska, Dustin Herbison, Elisa Bandy, Emma Wang, Eric Noland, Erica Moreira, Evan Senter, Evgenii Eltyshev, Francesco Visin, Gabriel Rasskin, Gary Wei, Glenn Cameron, Gus Martins, Hadi Hashemi, Hanna Klimczak-Plucińska, Harleen Batra, Harsh Dhand, Ivan Nardini, Jacinda Mein, Jack Zhou, James Svensson, Jeff Stanway, Jetha Chan, Jin Peng Zhou, Joana Carrasqueira, Joana Iljazi, Jocelyn Becker, Joe Fernandez, Joost van Amersfoort, Josh Gordon, Josh Lipschultz, Josh Newlan, Ju yeong Ji, Kareem

- Mohamed, Kartikeya Badola, Kat Black, Katie Millican, Keelin McDonell, Kelvin Nguyen, Kiranbir Sodhia, Kish Greene, Lars Lowe Sjoesund, Lauren Usui, Laurent Sifre, Lena Heuermann, Leticia Lago, Lilly McNealus, Livio Baldini Soares, Logan Kilpatrick, Lucas Dixon, Luciano Martins, Machel Reid, Manvinder Singh, Mark Iverson, Martin Görner, Mat Velloso, Mateo Wirth, Matt Davidow, Matt Miller, Matthew Rahtz, Matthew Watson, Meg Risdal, Mehran Kazemi, Michael Moynihan, Ming Zhang, Minsuk Kahng, Minwoo Park, Mofi Rahman, Mohit Khatwani, Natalie Dao, Nenshad Bardoliwalla, Nesh Devanathan, Neta Dumai, Nilay Chauhan, Oscar Wahltinez, Pankil Botarda, Parker Barnes, Paul Barham, Paul Michel, Pengchong Jin, Petko Georgiev, Phil Culliton, Pradeep Kuppala, Ramona Comanescu, Ramona Merhej, Reena Jana, Reza Ardeshtir Rokni, Rishabh Agarwal, Ryan Mullins, Samaneh Saadat, Sara Mc Carthy, Sarah Cogan, Sarah Perrin, Sébastien M. R. Arnold, Sebastian Krause, Shengyang Dai, Shruti Garg, Shruti Sheth, Sue Ronstrom, Susan Chan, Timothy Jordan, Ting Yu, Tom Eccles, Tom Hennigan, Tomas Kocisky, Tulsee Doshi, Vihan Jain, Vikas Yadav, Vilobh Meshram, Vishal Dharmadhikari, Warren Barkley, Wei Wei, Wenming Ye, Woohyun Han, Woosuk Kwon, Xiang Xu, Zhe Shen, Zhitao Gong, Zichuan Wei, Victor Cotruta, Phoebe Kirk, Anand Rao, Minh Giang, Ludovic Peran, Tris Warkentin, Eli Collins, Joelle Barral, Zoubin Ghahramani, Raia Hadsell, D. Sculley, Jeanine Banks, Anca Dragan, Slav Petrov, Oriol Vinyals, Jeff Dean, Demis Hassabis, Koray Kavukcuoglu, Clement Farabet, Elena Buchatskaya, Sebastian Borgeaud, Noah Fiedel, Armand Joulin, Kathleen Kenealy, Robert Dadashi, and Alek Andreev. Gemma 2: Improving open language models at a practical size, 2024.
- [70] Jason Wei, Xuezhi Wang, Dale Schuurmans, Maarten Bosma, Brian Ichter, Fei Xia, Ed H. Chi, Quoc V. Le, and Denny Zhou. Chain-of-thought prompting elicits reasoning in large language models. In Sanmi Koyejo, S. Mohamed, A. Agarwal, Danielle Belgrave, K. Cho, and A. Oh, editors, *Advances in Neural Information Processing Systems 35: Annual Conference on Neural Information Processing Systems 2022, NeurIPS 2022, New Orleans, LA, USA, November 28 - December 9, 2022*, 2022.
- [71] Sharath Turuvekere Sreenivas, Saurav Muralidharan, Raviraj Joshi, Marcin Chochowski, Ameya Sunil Mahabaleshwarkar, Gerald Shen, Jiaqi Zeng, Zijia Chen, Yoshi Suhara, Shizhe Diao, Chenhan Yu, Wei-Chun Chen, Hayley Ross, Oluwatobi Olabiyi, Ashwath Aithal, Oleksii Kuchaiev, Daniel Korzekwa, Pavlo Molchanov, Mostofa Patwary, Mohammad Shoeybi, Jan Kautz, and Bryan Catanzaro. Llm pruning and distillation in practice: The minitron approach, 2024.
- [72] Meta. Llama 3.2: Vision and Lightweight Models for Edge and Mobile Devices. <https://ai.meta.com/blog/llama-3-2-connect-2024-vision-edge-mobile-devices/>, January 2024. Accessed: 2025-03-14.
- [73] Tom Gunter, Zirui Wang, Chong Wang, Ruoming Pang, Andy Narayanan, Aonan Zhang, Bowen Zhang, Chen Chen, Chung-Cheng Chiu, David Qiu, Deepak Gopinath, Dian Ang Yap, Dong Yin, Feng Nan, Floris Weers, Guoli Yin, Haoshuo Huang, Jianyu Wang, Jiarui Lu, John Peebles, Ke Ye, Mark Lee, Nan Du, Qibin Chen, Quentin Keunebroek, Sam Wiseman, Syd Evans, Tao Lei, Vivek Rathod, Xiang Kong, Xianzhi Du, Yanghao Li, Yongqiang Wang, Yuan Gao, Zaid Ahmed, Zhaoyang Xu, Zhiyun Lu, Al Rashid, Albin Madappally Jose, Alec Doane, Alfredo Bencomo, Allison Vanderby, Andrew Hansen, Ankur Jain, Anupama Mann Anupama, Areeba Kamal, Bugu Wu, Carolina Brum, Charlie Maalouf, Chinguun Erdenebileg, Chris Dulhanty, Dominik Moritz, Doug Kang, Eduardo Jimenez, Evan Ladd, Fangping Shi, Felix Bai, Frank Chu, Fred Hohman, Hadas Kotek, Hannah Gillis Coleman, Jane Li, Jeffrey Bigham, Jeffery Cao, Jeff Lai, Jessica Cheung, Jiulong Shan, Joe Zhou, John Li, Jun Qin, Karanjeet Singh, Karla Vega, Kelvin Zou, Laura Heckman, Lauren Gardiner, Margit Bowler, Maria Cordell, Meng Cao, Nicole Hay, Nilesh Shahdarpuri, Otto Godwin, Pranay Dighe, Pushyami Rachapudi, Ramsey Tantawi, Roman Frigg, Sam Davarnia, Sanskruti Shah, Saptarshi Guha, Sasha Sirovica, Shen Ma, Shuang Ma, Simon Wang, Sulgi Kim, Suma Jayaram, Vaishaal Shankar, Varsha Paidi, Vivek Kumar, Xin Wang, Xin Zheng, Walker Cheng, Yael Shrager, Yang Ye, Yasu Tanaka, Yihao Guo, Yunsong Meng, Zhao Tang Luo, Zhi Ouyang, Alp Ayyar, Alvin Wan, Andrew Walkingshaw, Andy Narayanan, Antonie Lin, Arsalan Farooq, Brent Ramerth, Colorado Reed, Chris Bartels, Chris Chaney, David Riazati, Eric Liang Yang, Erin Feldman, Gabriel Hochstrasser, Guillaume Seguin, Irina Belousova, Joris Pelemans, Karen Yang, Keivan Alizadeh Vahid, Liangliang Cao, Mahyar Najibi, Marco Zuliani, Max Horton, Minsik Cho, Nikhil Bhendawade, Patrick

- Dong, Piotr Maj, Pulkit Agrawal, Qi Shan, Qichen Fu, Regan Poston, Sam Xu, Shuangning Liu, Sushma Rao, Tashweena Heeramun, Thomas Merth, Uday Rayala, Victor Cui, Vivek Rangarajan Sridhar, Wencong Zhang, Wenqi Zhang, Wentao Wu, Xingyu Zhou, Xinwen Liu, Yang Zhao, Yin Xia, Zhile Ren, and Zhongzheng Ren. Apple intelligence foundation language models, 2024.
- [74] NVIDIA. Tensorrt-llm. <https://github.com/NVIDIA/TensorRT-LLM>, 2023.
- [75] Jacob Devlin, Ming-Wei Chang, Kenton Lee, and Kristina Toutanova. BERT: pre-training of deep bidirectional transformers for language understanding. In Jill Burstein, Christy Doran, and Tamar Solorio, editors, *Proceedings of the 2019 Conference of the North American Chapter of the Association for Computational Linguistics: Human Language Technologies, NAACL-HLT 2019, Minneapolis, MN, USA, June 2-7, 2019, Volume 1 (Long and Short Papers)*, pages 4171–4186. Association for Computational Linguistics, 2019.
- [76] An Yang, Baosong Yang, Binyuan Hui, Bo Zheng, Bowen Yu, Chang Zhou, Chengpeng Li, Chengyuan Li, Dayiheng Liu, Fei Huang, Guanting Dong, Haoran Wei, Huan Lin, Jialong Tang, Jialin Wang, Jian Yang, Jianhong Tu, Jianwei Zhang, Jianxin Ma, Jianxin Yang, Jin Xu, Jingren Zhou, Jinze Bai, Jinzheng He, Junyang Lin, Kai Dang, Keming Lu, Keqin Chen, Kexin Yang, Mei Li, Mingfeng Xue, Na Ni, Pei Zhang, Peng Wang, Ru Peng, Rui Men, Ruize Gao, Runji Lin, Shijie Wang, Shuai Bai, Sinan Tan, Tianhang Zhu, Tianhao Li, Tianyu Liu, Wenbin Ge, Xiaodong Deng, Xiaohuan Zhou, Xingzhang Ren, Xinyu Zhang, Xipin Wei, Xuancheng Ren, Xuejing Liu, Yang Fan, Yang Yao, Yichang Zhang, Yu Wan, Yunfei Chu, Yuqiong Liu, Zeyu Cui, Zhenru Zhang, Zhifang Guo, and Zhihao Fan. Qwen2 technical report, 2024.
- [77] Ilya Loshchilov and Frank Hutter. Decoupled weight decay regularization. In *7th International Conference on Learning Representations, ICLR 2019, New Orleans, LA, USA, May 6-9, 2019*. OpenReview.net, 2019.
- [78] YiMing Liu. Rethinking kl divergence in rlhf: From single sample to mini-batch to expectation, 2025. Notion Blog.
- [79] Deepak Narayanan, Mohammad Shoeybi, Jared Casper, Patrick LeGresley, Mostofa Patwary, Vijay Korthikanti, Dmitri Vainbrand, Prethvi Kashinkunti, Julie Bernauer, Bryan Catanzaro, Amar Phanishayee, and Matei Zaharia. Efficient large-scale language model training on GPU clusters using megatron-lm. In Bronis R. de Supinski, Mary W. Hall, and Todd Gamblin, editors, *International Conference for High Performance Computing, Networking, Storage and Analysis, SC 2021, St. Louis, Missouri, USA, November 14-19, 2021*, page 58. ACM, 2021.
- [80] Jian Hu, Xibin Wu, Weixun Wang, Xianyu, Dehao Zhang, and Yu Cao. Openrlhf: An easy-to-use, scalable and high-performance RLHF framework. *CoRR*, abs/2405.11143, 2024.
- [81] Woosuk Kwon, Zhuohan Li, Siyuan Zhuang, Ying Sheng, Lianmin Zheng, Cody Hao Yu, Joseph E. Gonzalez, Hao Zhang, and Ion Stoica. Efficient memory management for large language model serving with pagedattention. In *Proceedings of the ACM SIGOPS 29th Symposium on Operating Systems Principles*, 2023.
- [82] Lianmin Zheng, Liangsheng Yin, Zhiqiang Xie, Chuyue Sun, Jeff Huang, Cody Hao Yu, Shiyi Cao, Christos Kozyrakis, Ion Stoica, Joseph E. Gonzalez, Clark Barrett, and Ying Sheng. Sglang: Efficient execution of structured language model programs, 2024.
- [83] Beijing Academy of Artificial Intelligence (BAAI). Infinity instruct. *arXiv preprint arXiv:2406.XXXX*, 2024.
- [84] Vijay Korthikanti, Jared Casper, Sangkug Lym, Lawrence McAfee, Michael Andersch, Mohammad Shoeybi, and Bryan Catanzaro. Reducing activation recomputation in large transformer models, 2022.

# Appendices

## A Dataset Analysis

Type-Token Rate (TTR), as a fundamental measure of lexical diversity, reflects the local variability of vocabulary, but it is sensitive to text length. The calculation formula is:

$$TTR = \frac{N_{types}}{N_{tokens}} \quad (7)$$

where  $N_{tokens}$  denotes the total number of 2-gram patterns in the text, and  $N_{types}$  represents the number of distinct 2-gram patterns.

Entropy, as an information-theoretic metric, quantifies the uncertainty within binary grammatical sequences based on their probability distribution. A higher entropy value indicates more complex local language patterns. The calculation formula is:

$$Entropy = - \sum_i^{N_{types}} p_i \log_2(p_i) \quad (8)$$

where  $p_i$  is the probability of occurrence for the  $i^{th}$  2-gram pattern.

Since both TTR and Entropy are sensitive to text length, to ensure a relatively fair comparison of dataset complexity, we randomly sample 700 entries from the test set of each dataset for calculation (as the ATIS dataset only contains 700 instances).

## B Details for Reinforcement Learning

Our reward design consists of two components, Format Reward( $S_{format}$ ) and Answer Reward( $S_{answer}$ ):

- For Format Reward, we adopt the logic of Logic-RL[9], which validates the output format against the specified template `<think>...</think><answer>...</answer>` via regular expressions. We add additional designs to ensure the validity of the usage of the function and its parameters. If a function not present in the predefined input function pool is selected, it is deemed invalid.

$$S_{format} = \begin{cases} 1, & \text{if the format is correct, and the function call is valid} \\ 0, & \text{otherwise} \end{cases} \quad (9)$$

- For Answer Reward, in our specific scenario, we observe that the model tends to directly guess answer during training, resulting in no association between the Chain-of-Thought (CoT) and the final results. Requiring explicit repetition of the answer within the CoT framework effectively resolves this issue. As illustrated in Figure 6, we optimize its original design in order to enhance the consistency between the Chain-of-Thought (CoT) reasoning and the results. Our requirements are as follows: (1) The CoT must explicitly reference the target function at least once; (2) The final function mentioned in the CoT must correspond to the function in the answer. Failure to comply with these conditions will be regarded as a parsing error. Additionally, we incorporate fine-grained rewards, which provide better guidance when the answer is partially correct, enabling the model to achieve improved performance.

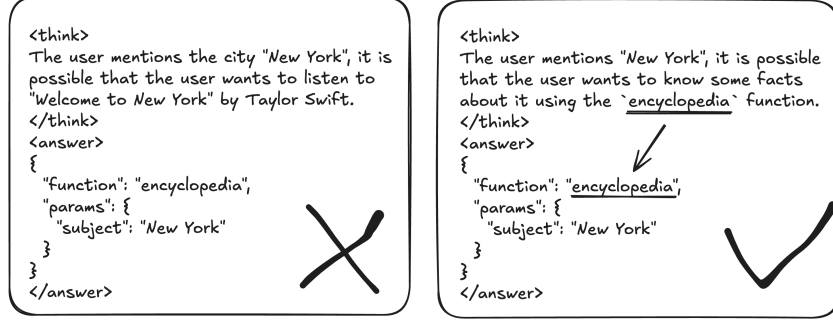


Figure 6: An example of optimization of the original Answer Reward design by requiring explicit repetition of the answer within the CoT framework.

$$S_{\text{answer}} = \begin{cases} -2 & \text{if the answer is missing, or is unable to be parsed,} \\ & \text{or is not defined in the function list,} \\ & \text{or the thought doesn't end with the function in the answer} \\ -1.25 & \text{if the names of at least one parameter and function are correct,} \\ -1.2 & \text{if the name of function, as well as the name} \\ & \text{and value of at least one parameter are correct} \\ 2, & \text{if the answer is correct,} \\ -1.5, & \text{otherwise} \end{cases} \quad (10)$$

## C Prompt Compression

To reduce inference costs, we remove unnecessary content in prompts, such as guidelines, format specifications, and few-shot examples used during large model invocation, while retaining essential elements: user queries, context, query-relevant knowledge, function lists, and brief function descriptions. For outputs, we remove Chain-of-Thought (CoT) components and directly use predefined JSON-formatted responses, as illustrated in Figure 7.

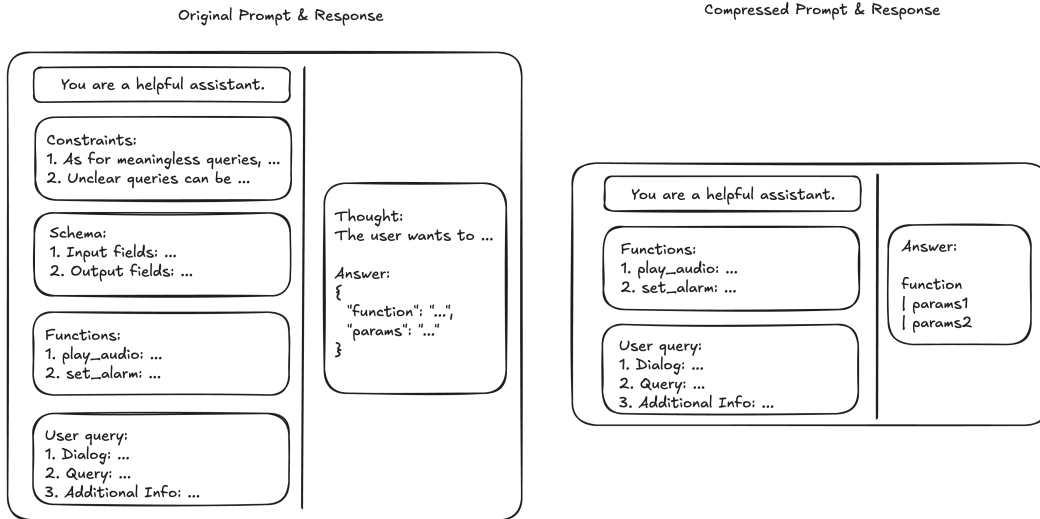


Figure 7: Original vs Compressed Prompt & Response.

## D Retriever Setup

Initially, we select GTE-large [63], which is trained on the BERT-large [75], as our embedding model. Using this model, we generate embeddings of API descriptions produced by the LLMs. Then, we compare these embeddings with those of the API description from the document using cosine similarity. However, this model’s recall accuracy is not high. Subsequently, we switch to GTE-Qwen2-1.5B-instruct [63], a model trained on Qwen2-1.5B [76], which offers the advantage of fine-tuning for matching tasks through prompt modification. Next, utilizing this model with a customized prompt in Section D.1, we perform cosine similarity matching between the model-generated API descriptions and the JSON text of the entire API documentation, achieving a higher accuracy. During training, we optimize the API description model using rejection sampling, with implementation details provided in Section D.2. Finally, to achieve optimal inference acceleration, we train a classifier based on BERT-large [75] for top-1 recall using rejection sampling. The classifier takes Dialog, User Query, and necessary context as input and the function category as output. The functions corresponding to the top-k output logits are then considered as candidate functions for the subsequent model’s function call. This approach significantly accelerates inference due to the efficiency of BERT classifiers compared to autoregressive GPT models, while also enhancing function recall capabilities. However, it introduces scalability challenges since the recall model needs to be retrained with each update to the function pool. As illustrated in Table 5, this series of optimizations lead to a substantially improvement in API recall rates.

Table 5: Comparison of retrieval performance of models: GTE-large model, GTE-Qwen2-1.5B-instruct model, optimized API description model + GTE-Qwen2-1.5B-instruct model. Extensibility implies that the API pool can be dynamically modified.

Top-N	GTE-large	GTE-Qwen2	Opt-API+GTE-Qwen2	RFT-BERT
5	60.19%	88.27%	93.39%	99.61%
7	74.06%	94.67%	98.09%	99.92%
10	90.11%	98.22%	99.55%	99.92%
15	98.95%	99.80%	100%	100%
Extensibility	✓	✓	✓	×

### D.1 Prompt for retrieval

Instruction: Given a API description, retrieve the most similar API from the function pool.  
Query:

### D.2 Retriever Optimization

---

#### Algorithm 1 Simplified API Description Validation Process

---

**Require:** Query  $q$ , LLM  $\mathcal{M}$ , API Pool  $\mathcal{R}$ , Retrieval Module  $\mathcal{S}$ , Function Call Module  $\mathcal{F}$ , Judge  $\mathcal{J}$

**Ensure:** High-quality training dataset  $\mathcal{D}$

- 1: Generate multiple API descriptions  $Des = \{\mathcal{M}(q)\}$  in parallel.
  - 2: **for** each description  $d \in Des$  **do**
  - 3:   Retrieve candidate APIs  $C = \mathcal{S}(d, \mathcal{R})$ .
  - 4:   Select API  $a \in C$  and generate parameters  $p$ .
  - 5:   Execute  $a$  with  $p$ , get result  $r$ .
  - 6:   **if**  $\mathcal{J}(r) = \text{Success}$  **then**
  - 7:     Check if  $a$  is in the top 5 candidates of  $C$ .
  - 8:     **if** Yes **then**
  - 9:       Add  $(q, d, a, p, r)$  to  $\mathcal{D}$ .
  - 10:    **end if**
  - 11:   **end if**
  - 12: **end for**
-



Table 6: Training Parameters in different phases.

Supervised Fine-tuning (SFT)	
Learning Rate	$2 \times 10^{-5}$
Batch Size	128
Number of Epochs	1
Weight Decay	$1 \times 10^{-4}$
Reinforcement Learning (RL)	
Learning Rate	$3 \times 10^{-7}$
Batch Size	128
Number of Episodes	1400
Number of Rollouts	8
KL Coefficient	0.001
Knowledge Distillation (KD)	
Learning Rate	$2 \times 10^{-5}$
Batch Size	128
Number of Epochs	1
Logits Top-K	100

Table 7: Different KD results on Qwen2.5-0.5B model.

Model	AR
Qwen2.5-0.5B (RFT)	94.66%
Qwen2.5-0.5B (FKL)	94.65%
Qwen2.5-0.5B (AKL) $ \mu = 0.5$	94.48%
Qwen2.5-0.5B (AKL) $ \mu = 0.7$	94.68%
Qwen2.5-0.5B (AKL) $ \mu = 0.9$	<b>94.85%</b>

## E Training Details

The main training parameters are detailed in Table 6. During the training phase, we employ the AdamW optimizer [77], setting the model’s maximum sequence length to 5120. In the RL phase, we utilize the baseline variant of Reinforce++ [50] as the reinforcement learning algorithm, offering advantages in efficiency, conciseness, and training stability. Following [78], the K2 estimator is used instead of the original K1 in Reinforce++. In the AKL phase, the threshold parameter  $\mu$  is reduced from 1 to 0.5. For pruning, we use the 0.5B-Instruct model as the base, implementing width/depth pruning strategies with a 20%/30% prune ratio, resulting in two models Qwen2.5-0.4B(0.35B)-Width and Qwen2.5-0.4B(0.35B)-Depth. These extremely compressed models are produced through a two-phase training process involving accuracy recovery training and knowledge distillation (KD). Comprehensive training details for the pruned models are available in Appendix I. For quantization, we primarily experiment with three strategies on the 0.5B model trained with AKL: W8A16, W4A16, and W8A8. Both W8A16 and W4A16 employ per-group symmetric int8 weight-only quantization with a group\_size=128, while activations are in fp16. To improve accuracy, W4A16 use 512 training data samples combined with the GPTQ algorithm [33] for calibration. In contrast, W8A8 uses FP8 for both weights and activations. For the training frameworks, we utilize Megatron-LM [79] for SFT and KD, while OpenRLHF [80] is employed for RL. Data sampling during training is conducted using vLLM [81]. In the evaluation phase, we employ SGLang [82] to generate data.

## F Computing resources

We utilize 8 NVIDIA H20 GPUs for training and data generation processes. For evaluating inference performance, a single NVIDIA L20 GPU is employed. We apply an INTEL XEON PLATINUM 8575C processor with 192 cores for computation, operating at a frequency of 3028.956 MHz and a cache size of 327680 KB. Additionally, we establish a virtual development environment based on Kubernetes, leveraging 64 virtual cores and 512 GB of memory. During the training phase, the RFT process spans approximately 2 to 14 hours for models ranging from 0.5B to 7B in size. Pre-KD logits caching for a 7B model requires about 5 hours, whereas RL for the 3B model extends to approximately 3 days. The KD process for the 0.5B model is completed within about 2 hours, and training each pruned model requires roughly 3.5 days. Moreover, for the LLM prototype and LLM-as-a-Judge, generating data for every 10,000 entries takes approximately 1 hour.

## G Detailed Analysis for Experimental Results for KD

As demonstrated in Table 7, it is clear that balancing FKL and RKL is crucial for our task. The function selection process by the model resembles a classification task, whereas generating parameter names and values for function calls is more akin to a generation task. The parameter  $\mu$  in AKL is precisely used to adjust the effects between classification and generation. Experimental results demonstrate that at  $\mu \leq 0.7$  and  $\mu = 1.0$  (equivalent to FKL), the performance with AKL is similar to or worse than RFT. Based on our findings where the average probability of the top-1 token from the teacher model exceeds 99%, we conclude that setting a lower  $\mu$  value causes the effect of AKL to excessively shift more towards RKL. As described in the AKL paper, RKL prioritizes learning the tail of the probability distribution, which can impede rapid convergence in scenarios without requiring diversity. However, RKL can bring considerable benefits for the function classification part. Overall, AKL demonstrates greater potential compared to RFT, achieving performance improvements with an appropriately chosen  $\mu$  value.

## H Inference Details

The inference framework utilizes TensorRT-LLM[74] v0.16.0 with enabled optimizations including paged attention, prefix cache, CUDA graph size set to 1024, and max token number set to 32768 for inference acceleration.

## I Pruning Details

### I.1 Offline One-shot Pruning

**Importance as Metric for Structured Pruning** For Depth Pruning, we adopt Layer Importance (LI) as the metric, which is based on the similarity between consecutive layers' activation. Formally, we define the importance of the  $i$ -th layer as:

$$LI_i = 1 - \mathbb{E}_{X,t} \frac{X_{i,t}^T X_{i+1,t}}{\|X_{i,t}\|_2 \|X_{i+1,t}\|_2} \quad (11)$$

where  $X_i$  denotes the activation matrix of the  $i$ -th layer and  $X_{i,t}$  denotes the  $t$ -th column (embedding vector) of  $X_i$ . After all layer activations  $\{X_i\}_{i=1}^L$  through a single forward pass on calibration data are collected, the  $N$  least important layers are removed, where  $N$  is determined by the target pruning ratio. For Width Pruning, we classify width pruning into three dimensions based on channel dependencies: Embedding dimension, Head dimension and Intermediate dimension (as illustrated in Figure 8). For compact LLMs (e.g., Qwen2.5-0.5B with head size of 14), we exclude head dimension pruning due to its demonstrated sensitivity[37]. Instead, we employ an activation-based importance metric, Channel Importance(CI), for channel selection as follows:

$$CI_{\text{embedding}}^i = \sqrt{\sum_{b,s} |\text{LN}(X)^i|^2}, \quad CI_{\text{inter}}^i = \sqrt{\sum_{b,s} |x(W_{ffn1}^i)^T|^2} \quad (12)$$

where  $CI_{\text{embedding}}^i$  denotes the importance score of the  $i$ -th embedding dimension, computed from the LayerNorm outputs of attention and FFN blocks, while  $CI_{\text{inter}}^i$  denotes the importance of the  $i$ -th intermediate dimension, calculated from the  $i$ -th row of FFN's gate and up projection matrices  $W_{ffn1}^i$ . The importance scores are first aggregated across batch and sequence dimensions through summation  $\sum_{b,s}$ , then normalized using L2 normalization within each subgroup to obtain global channel importance.

Table 8: Perplexity (PPL) on WikiText-2 for different model architectures with 20% and 30% width pruning.

Model	Hidden Size	FFN Inter Size	Non-Emb Params(B)	Emb Param(B)	Params (B)	WikiText2 PPL
Qwen2.5-0.5B	896	4864	0.358	0.136	0.345	14.28
Qwen2.5-0.4B-Width-1	896	3328	0.259	0.136	0.395	349.89
Qwen2.5-0.4B-Width-2	832	3840	0.271	0.126	0.397	<b>251.95</b>
Qwen2.5-0.4B-Width-3	768	4352	0.278	0.117	0.395	354.74
Qwen2.5-0.4B-Width-4	706	4864	0.282	0.107	0.389	493.55
Qwen2.5-0.35B-Width-1	896	2560	0.209	0.136	0.345	1210.42
Qwen2.5-0.35B-Width-2	768	3584	0.236	0.117	0.351	1141.69
Qwen2.5-0.35B-Width-3	768	3584	0.236	0.117	0.353	<b>1009.57</b>
Qwen2.5-0.35B-Width-4	706	4096	0.242	0.107	0.349	2026.00
Qwen2.5-0.35B-Width-5	640	4864	0.256	0.097	0.353	2395.52

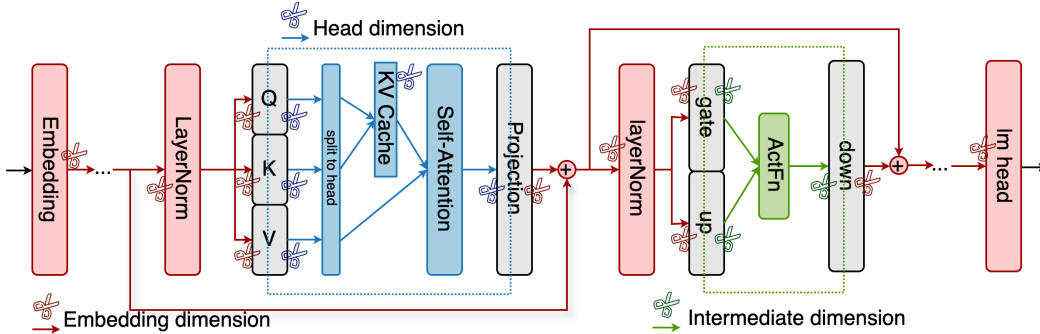


Figure 8: Pruning Dependency in the Qwen2.5

**Optimal Width Pruning Configuration** To ensure hardware-efficient matrix multiplication during inference, we set the pruning granularity to 64 for embedding dimension and 256 for the intermediate dimension. This approach results in multiple width-pruned model configurations, as show in Table 8. We calculate channel importance scores  $CI_{\text{embedding}}^{(i)}$  and  $CI_{\text{inter}}^{(j)}$  using a calibration dataset consisting of 1024 randomly sampled sequences from WikiText-2. For each configuration, we prune entire channel groups with the lowest CI scores and evaluate the resulting one-shot pruned models through WikiText-2 perplexity. Table 8 presents the optimal configurations for width pruning at rates of 20% and 30%, identified as Qwen2.5-0.4B-Width-2 and Qwen2.5-0.35B-Width-3, respectively.

## I.2 Recovery Training in Pruning

**Recovery Training Dataset and Hyperparameters** We use the Infinity-Instruct-7M[83] dataset and apply AKL distillation[29] described in Section 3.2 for general instruction recovery training. Qwen2.5-7B-Instruct[11] serves as the teacher model, and we follow Minitron’s methodology[71] to perform teacher correction on the Infinity-Instruct-7M dataset. The Adam optimizer is used with a weight decay of  $1e-4$  in conjunction with a cosine learning rate schedule, decaying from  $2e-5$  to  $2e-6$ . We conduct training over 2 epochs, utilizing a batch size of 32, with each batch packed to accommodate sequences of up to 7168 tokens.

Table 9: Performance comparison of Qwen2.5 models after pruning. We report 5-shot performance on mmlu and cmmlu, 4-shot for gsm8k, zero-shot for ARC-Challenge, HellaSwag. \* denotes that the baseline Qwen-2.5-0.5B utilizes the same instruct fine-tuning dataset for correction.

Model	MMLU 5-shot	CMMLU 5-shot	Arc-C 0-shot	HellaSwag 0-shot	GSM8k 4-shot	Avg.
Qwen-2.5-0.5B*	44.65	42.53	50.17	39.13	45.11	44.32
Qwen-2.5-0.4B-Width	38.63	35.89	42.27	35.55	48.60	40.12
Qwen-2.5-0.35B-Width	35.85	33.18	40.21	32.21	44.35	37.16
Qwen-2.5-0.4B-Depth	32.89	32.41	37.11	33.69	37.68	34.76
Qwen-2.5-0.35B-Depth	25.46	24.42	26.12	25.21	5.61	21.36

**Performance across Knowledge Assessment & Reasoning Tasks** Table 9 summarizes the performance of pruned models across various downstream tasks, including MMLU and CMMLU for knowledge assessment, alongside ARC-Challenge, HellaSwag and Winogrande for commonsense reasoning evaluation. Our experiments reveal distinct recovery patterns between width and depth pruning across general tasks. At a 20% pruning rate, width pruning achieves 90.5% of the performance relative to the unpruned baseline, while depth pruning retains only 78.4%. When increasing the pruning intensity to 30%, width pruning preserves 83.8% of the original performance. In contrast, depth pruning suffers catastrophic performance degradation, particularly on the GSM8K task, where accuracy drops from 45.11 to a merely 5.61.

#### Ablation of Pruning Ratio on Domain-Specific Task

Our investigation reveals a nonlinear relationship between pruning intensity and model accuracy in domain-specific tasks. As shown in Table 10, both depth-wise and width-wise pruning at a 20% pruning rate result in a negligible <0.5% AR reduction. However, increasing the pruning rate to 30% leads to notable performance deterioration (>1.5% AR drop). These findings suggest that for small-scale models on domain-specific tasks, pruning rates exceeding 20% may significantly compromise accuracy.

Table 10: Results with different pruning strategies on domain specific tasks.

Model	AR
Qwen2.5-0.5B (KD)	94.85%
Qwen2.5-0.4B-Width (KD)	94.17%
Qwen2.5-0.35B-Width (KD)	93.71%
Qwen2.5-0.4B-Depth (KD)	94.20%
Qwen2.5-0.35B-Depth (KD)	93.75%

## J FLOPs Calculation

For the calculation of FLOPs, we first define the notations symbolically:

- $b$ : the batch size
- $h$ : the hidden size
- $s_t$ : the total average number of prompt tokens
- $s_u$ : the average number of uncached tokens in prefill phase
- $n_a$ : the number of attention heads
- $n_{kv}$ : the number of separate key/value heads in GQA
- $d_h$ : the dimension of each head
- $d_i$ : the intermediate dimension of FFN layer
- $v$ : the vocabulary size
- $l$ : the number of model layers

According to [84], we calculate the floating-point operations (FLOPs) of the Qwen2.5 models, only considering matrix multiplications (GEMMs) without norms and activations:

- **Attention block operations:**
  - Query/Key/Value transformations (GQA):  $2bs_uhd_h(n_a + 2n_{kv})$
  - Attention matrix computation and attention over values:  $2bs_t s_u n_a d_h$
  - Post-attention linear projection:  $2bs_u h n_a d_h$
- **Feed-forward network block operations:**

- Up/Gate/Down projections (each):  $2bs_uhd_i$
- **LM head operations:**  $2bhv$

Thus, the total FLOPs for one inference with prefill cache is:

$$\text{FLOPs}_{\text{total}} = l \left[ 4bs_uhd_h(n_a + n_{kv}) + 2bs_us_td_hn_a + 6bs_uhd_i \right] + 2bhv$$

**Workload and Computational Analysis** We conduct experiments on our datasets, in which prompts have an average length of 1792 tokens. By leveraging prefix caching to exploit shared prompt prefixes during inference, we reduce the average number of uncached tokens in the prefill phase to 128 and generate an average of 9 tokens per request. We calculate FLOPs under  $s_u = 128$  tokens in the prefill phase and under  $s_u = 1$  token for each step in the decoding phase, with detailed results presented in [Table 2](#).

## K Extensive Attempts on Generalization Enhancement via RL

Table 11: Full results during the RL exploration

Model	AR (In-Domain)	AR (Out-of-Domain)
Crowdsourced Labelers	77.85%	-
BERT-based System	81.43%	-
Qwen2.5-72B (ICL)	94.74%	<u>94.63%</u>
Qwen2.5-7B (RFT)	95.29%	90.86%
Qwen2.5-3B (RFT)	95.30%	91.02%
Qwen2.5-0.5B (RFT)	94.66%	90.62%
Qwen2.5-0.5B (KD)	94.66%	90.62%
Qwen2.5-7B (RL)	<u>95.36%</u>	<b>94.80%</b>
Qwen2.5-3B (RL)	94.68%	92.94%
Qwen2.5-0.5B (RL)	90.76%	85.21%
Qwen2.5-0.5B (KD*)	88.49%	84.14%
Qwen2.5-0.5B (KD*+RL)	<b>95.55%</b>	91.68%

While attempting to apply reinforcement learning (RL), we conduct extensive experiments, with results shown in [Table 11](#). Initially, we find that directly training a 7B model with RL yields excellent results, surpassing the LLM Prototype and RFT-trained models. Subsequently, we attempt to train smaller models (3B and 0.5B) and discover that RL is ineffective on the 0.5B model, because the model tends to generate shorter or even meaningless Chain-of-Thought (CoT), leading to degraded output diversity as well as that without CoT. To address the issue above, we explore another approach, transferring out-of-domain capabilities into the 0.5B model via Knowledge Distillation (KD). However, we observe that the model struggles with format errors due to underfitting. Ultimately, after applying RL training on this model, we notice an impressive improvement on model performance, with both an absolute 1% AR increase on in-domain/out-of-domain datasets compared to the 0.5B RFT-trained model.